Sedimentary Geology 296 (2013) 103–121

Contents lists available at ScienceDirect

Sedimentary Geology

journal homepage: www.elsevier.com/locate/sedgeo

Sedimentology and palaeontology of the Upper Jurassic Puesto Almada Member (Cañadón Asfalto Formation, Fossati sub-basin), Patagonia Argentina: Palaeoenvironmental and climatic significance ☆

Nora G. Cabaleri [a], Cecilia A. Benavente [b,*], Mateo D. Monferran [c], Paula L. Narváez [b], Wolfgang Volkheimer [b], Oscar F. Gallego [c], Margarita D. Do Campo [a]

[a] Instituto de Geocronología y Geología Isotópica (INGEIS), Consejo Nacional de Investigaciones Científicas y Técnicas (CONICET), Universidad de Buenos Aires, Ciudad Universitaria, C1428EHA Buenos Aires, Argentina
[b] Instituto Argentino de Nivología, Glaciología y Ciencias Ambientales (IANIGLA), CCT-CONICET-Mendoza, Av. Adrián Ruiz Leal s/n, Parque General San Martín, 5500 Mendoza, Argentina
[c] Micropaleontología, Facultad de Ciencias Exactas y Naturales y Agrimensura, Universidad Nacional del Nordeste (UNNE), Área Paleontología, Centro de Ecología Aplicada del Litoral (CECOAL), CCT-CONICET-Nordeste, C.C.128, 3400 Corrientes, Argentina

ARTICLE INFO

Article history:
Received 9 May 2013
Received in revised form 20 August 2013
Accepted 21 August 2013
Available online 28 August 2013

Editor: B. Jones

Keywords:
Facies
Palaeontology
Palaeoclimatology
Upper Jurassic
Cañadón Asfalto Formation
Patagonia

ABSTRACT

Six facies associations are described for the Puesto Almada Member at the Cerro Bandera locality (Fossati sub-basin). They correspond to lacustrine, palustrine, and pedogenic deposits (limestones); and subordinated alluvial fan, fluvial, aeolian, and pyroclastic deposits. The lacustrine–palustrine depositional setting consisted of carbonate alkaline shallow lakes surrounded by flooded areas in a low-lying topography. The facies associations constitute four shallowing upward successions defined by local exposure surfaces: 1) a Lacustrine–Palustrine-pedogenic facies association with a 'conchostracan'–ostracod association; 2) a Palustrine facies association representing a wetland subenvironment, and yielding 'conchostracans', body remains of insects, fish scales, ichnofossils, and palynomorphs (cheirolepidiacean species and ferns growing around water bodies, and other gymnosperms in more elevated areas); 3) an Alluvial fan facies association indicating the source of sediment supply; and 4) a Lacustrine facies association representing a second wetland episode, and yielding 'conchostracans', insect ichnofossils, and a palynoflora mainly consisting of planktonic green algae associated with hygrophile elements. The invertebrate fossil assemblage found contains the first record of fossil insect bodies (Insecta-Hemiptera and Coleoptera) for the Cañadón Asfalto Formation. The succession reflects a mainly climatic control over sedimentation. The sedimentary features of the Puesto Almada Member are in accordance with an arid climatic scenario across the Upper Jurassic, and they reflect a strong seasonality with periods of higher humidity represented by wetlands and lacustrine sediments.

1. Introduction

The Jurassic basins of Patagonia are associated with intense volcanism and plutonism, which was the result of subduction at the western margin. In the Middle Jurassic, magmatic activity became particularly intense in Patagonia as well as in several other areas of Gondwana (Spalletti and Franzese, 2007). The Cañadón Asfalto Basin was characterized by a great diversity of environments, represented mainly by lakes, rivers, ponds, and wetlands, which suffered dry and wet intervals and which were affected by magmatic activity (Lizuain and Silva Nieto, 1996; Cabaleri and Armella, 1999; Cabaleri et al., 2010a; Gallego et al., 2011).

The sedimentological study of carbonate deposits is relevant since these deposits contain high resolution information about climatic conditions at the time of deposition (Platt and Wright, 1992). The Cañadón Asfalto Formation in the Fossati sub-basin, possesses thick limestone beds that allow such studies. The limestones of the lower member of this formation, the Las Chacritas Member, were recently studied by Cabaleri and Benavente (2013). The sedimentary features revealed an intermediate climate (arid to sub-humid conditions) and suggested that minor sedimentary changes were caused by variations in the exposure index of the Las Chacritas wetland directly determined by climatic conditions. The upper member of the unit, the Puesto Almada Member, has also numerous limestone beds that have not yet been studied and that could provide valuable information about the dynamics of the sedimentary system that could be extrapolated to the other sub-basins of the Cañadón Asfalto Basin. Therefore our objective in this paper is to complete the palaeoenvironmental framework, based on sedimentological, mineralogical, and palaeontological data, at the time of deposition of the upper section of the Cañadón Asfalto Formation (i.e., the Puesto Almada Member), outcropping at the Cerro Bandera locality (Fig. 1). With the information provided by the aforementioned proxies, the palaeogeographic setting, and other relevant reports, we aim

☆ In memory of Dr. Sara Ballent (1950–2011).
* Corresponding author.

0037-0738/$ – see front matter © 2013 Elsevier B.V. All rights reserved.
http://dx.doi.org/10.1016/j.sedgeo.2013.08.011

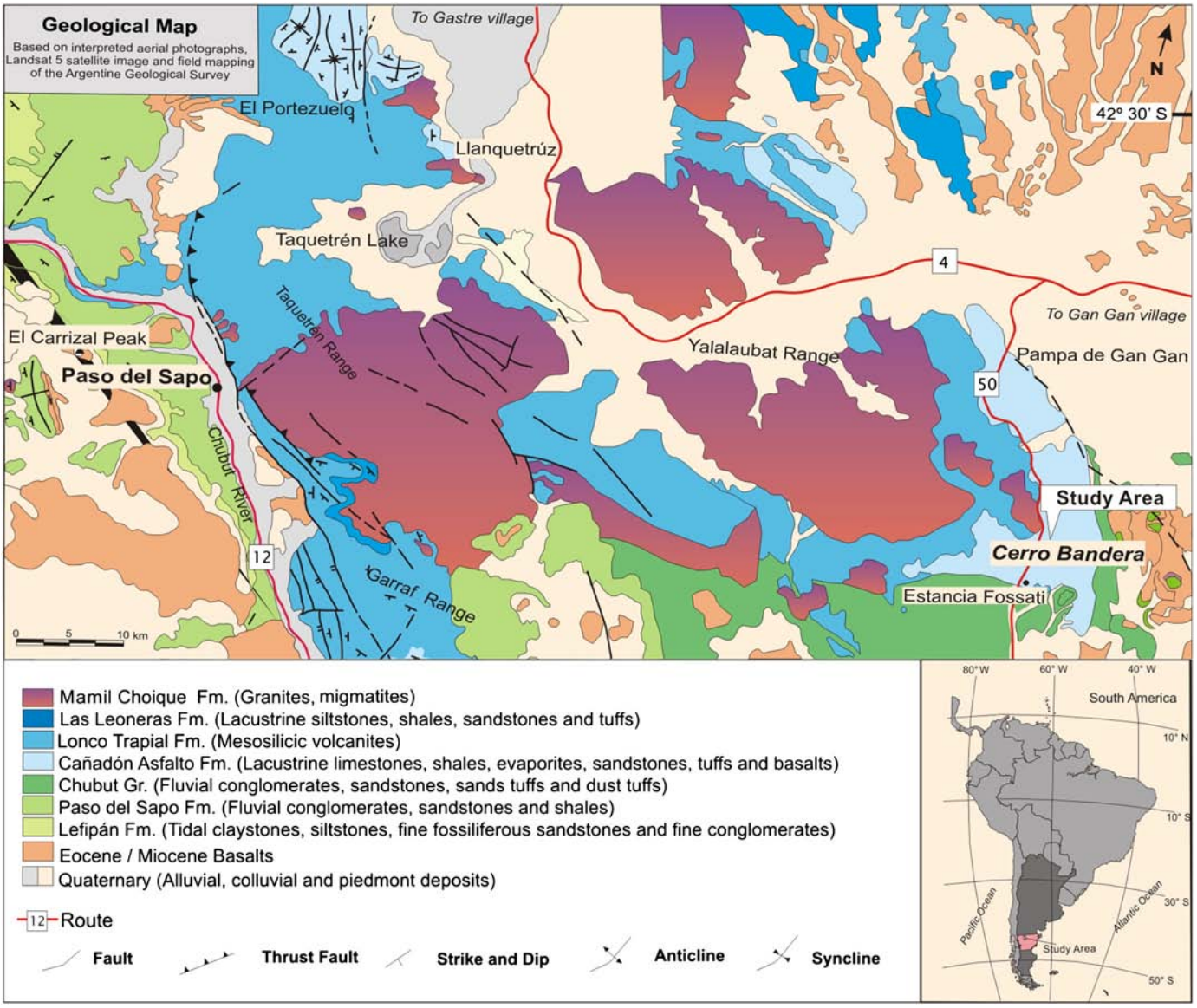

Fig. 1. Location and geological map of the Cerro Bandera locality in the Fossati sub-basin showing the outcropping units (Permian through Quaternary) modified from Cabaleri and Benavente (2013).

to contextualize the studied succession within the Late Jurassic palaeoclimatic conditions of southern South America.

2. Geological setting

A detailed geologic framework of the Cañadón Asfalto Basin is presented in Cabaleri et al. (2010a) and Cabaleri and Benavente (2013). Three sub-basins are recognized as part of the Cañadón Asfalto Basin: Cerro Cóndor (middle Chubut River area), El Portezuelo-Llanquetrúz (NW of Gastre village) (Figari et al., 1996), and Fossati (Pampa de Gan Gan) (Silva Nieto et al., 2007). Stratigraphic descriptions of the Cerro Cóndor and Fossati sub-basins are given by Cabaleri et al. (2006, 2008, 2010a, 2011).

The Fossati sub-basin occupies the north central region of the Cañadón Asfalto rift basin, formed by NW oriented faults (see Fig. 1 in Cabaleri and Benavente, 2013). The basement of the Fossati sub-basin is represented by the Mamil Choique Formation (Ravazzoli and Sesana, 1997), with a radiometric K/Ar age of 249.7 ± 5.3 Ma that corresponds to Permian–Triassic. This unit is unconformably covered by the Las Leoneras Formation (Pliensbachian age, 188.946 ± 0.096/0.13/0.24 Ma; Cúneo et al., 2013), which underlies the Lower–Middle Jurassic volcanites (K/Ar 173.1 ± 9.4 Ma; Silva Nieto, 2005) from the Lonco Trapial Formation (Lesta and Ferello, 1972), with an unconformity at the basal contact. The Lonco Trapial Formation is then unconformably overlain by the Cañadón Asfalto Formation, which is in turn separated from the continental deposits of the Chubut Group (Los Adobes and Cerro Barcino formations; Barremian–Santonian) by a low-angle unconformity. The Chubut Group (Lesta, 1968; Codignotto et al., 1979) was formed during a stage of tectonic stability (*sag* stage) (Ranalli et al., 2011). In the eastern area of the Cerro Bandera locality (Fig. 1), the Cañadón Asfalto Formation is covered by the Paso del Sapo (Campanian/Maastrichtian) and Lefipán formations (Lesta and Ferello, 1972). The Paleogene is represented by the Salamanca Formation and by the Eocene–Miocene basalts (Fig. 1).

The Cañadón Asfalto Formation (Stipanicic et al., 1968) is one of the most significant units of the basin. It is a thick sedimentary succession that includes lacustrine and fluvial systems, pyroclastic intercalations, and olivine-rich basalt flows at its base (Stipanicic et al., 1968; Nullo, 1983; Turner, 1983; Cabaleri et al., 2010a). The age of the complete volcano-sedimentary unit is Toarcian–Aalenian to Tithonian

(Salani, 2007; Cabaleri et al., 2010b). It is composed of two members: Las Chacritas (Aalenian to the Early Bajocian) and Puesto Almada (Late Callovian–Oxfordian to Tithonian) (Cabaleri et al., 2010a,b). Both members of the Cañadón Asfalto Formation outcrop within the Fossati sub-basin.

Overlying the Las Chacritas Member, the Puesto Almada Member represents the Late Callovian–Tithonian according to a U/Pb age of 161 ± 3 Ma from a tuff layer of the section at the Estancia La Sin Rumbo locality (Cerro Cóndor sub-basin) (Cabaleri et al., 2010b; Gallego et al., 2011). At the Cerro Bandera locality, a U/Pb age of 158 ± 1 Ma (Hauser et al., 2012) was obtained from a tuff layer of that member.

At its type locality, Estancia El Torito (Cerro Cóndor sub-basin), the Puesto Almada Member is mainly represented by tuffs and tuffites, interbedded with brown yellowish laminated limestones that contain fish and plant remains. Cabaleri et al. (2010a) analysed the type locality: the dark grey limestone beds have ripple cross-stratification and mud cracks that are interbedded with thin layers of blue shales and argillaceous limestones with 'conchostracans'. The lower section of the unit contains medium grained, grey-to-white sandstones with carbonate cementing, with planar cross-bedding commonly observed. In the same layers, there are silicified tree trunks, both upright and fallen. These layers are overlain by tuffs, tuffites, and red laminated sandstones. At the time of deposition, the sediment supply outpaced the rate of the tectonic activity with differential subsidence controlled by faulting, causing the deposition of well-sorted, coarse clastic sediments in shallow lacustrine basins and wetlands, with pyroclastic materials also present (Cabaleri et al., 2010a). The main characteristic of the unit is the presence of rhythmites with fish remains. Also, the fossil record includes 'conchostracans': Eosestheriidae, *Congestheriella rauhuti* Gallego, Shen, Cabaleri and Hernandez, *Pseudestherites* sp., and *Euestheria*?; bivalves: cf. *Diplodon*; gastropods: "Viviparus"?; ostracods: *Theryosinoecum barrancalensis minor* Musacchio, Beros and Pujana, *Penthesilenula sarytirmenensis* (Sharapova), *Timiriasevia* sp., and *Metacypris* sp.; and caddisflies (Musacchio et al., 1990; Musacchio, 1995; Gallego and Cabaleri, 2005; Martínez et al., 2007; Monferran et al., 2008; Gallego et al., 2010).

3. Materials and methods

The Puesto Almada Member outcrops studied here come from the Cerro Bandera locality, NW of the El Escorial village (42° 48′ 9.7″S and 68° 29° 1.5″W) (Fig. 1). They cover a belt 5000 m long and 2000 m wide, with a stratigraphic thickness of about 70 m (Fig. 2). Field description included recording of the various characteristics of the beds in vertical succession such as dimensions, colour, and lithology. Lateral variations were also described when found, reflecting changes in the sedimentation. We performed sampling from a limestone section following Flügel (2004), with 54 samples collected at a centimetre scale, and with 18 additional samples collected from each of the previously defined microfacies. Carbonate samples were sent to the Rock Cutting and Thin Sectioning Laboratory of the Instituto de Geocronología y Geología Isotópica (INGEIS) for production of polished slabs and standard thin sections (7.5 cm^2). The polished slabs were described using a low-magnification stereo microscope (Leica S8 APO). Thin sections were stained with Alizarin Red S to differentiate calcite from dolomite, and were observed and photographed using a Zeiss Axioskop 40 petrographic microscope. Microfacies were labelled using the abbreviation PAF followed by an identifying number.

Claystone and siltstone samples were collected for X-ray diffraction (XRD) bulk and clay-mineral analysis of the under 2 μm fraction. The mineralogical compositions of 17 siltstones and claystones were determined by XRD at the INGEIS laboratory, using a Philips PW1050 diffractometer with Cu*K*α radiation, operated at 40 mA and 30 kV. Clay sub-samples (<2 μm) were prepared in accordance with Moore and Reynolds (1997). Calcium carbonate was removed from the samples using an acetic acid–sodium acetate buffer (pH = 5), prior to clay separation by centrifugation. Clay minerals were identified according to the position of the (00 l) series of basal reflections on XRD patterns from air-dried, ethylene-glycolated samples, heated at 500 °C for 4 h.

The palynological samples were collected from two intervals of the exposed units (14.0–23.8 m and 32.4–43.0 m; Figs. 2, 3), with six samples yielding palynomorph assemblages (Fig. 3). The physical/chemical extraction of palynomorphs was performed in the Palaeopalynology Laboratory of the Instituto Argentino de Nivología, Glaciología y Ciencias Ambientales (IANIGLA). Samples were treated with hydrochloric and hydrofluoric acids using the standard palynologic processing techniques described in Volkheimer and Melendi (1976). The palynological slides were examined under an Olympus BX50 transmitted light microscope fitted with a digital camera, and the material was also analysed using scanning electron microscopy (SEM) at the Museo Argentino de Ciencias Naturales "Bernardino Rivadavia" (MACN) in Buenos Aires. The slides produced are stored in the Palaeopalynology Collection (MPLP: Mendoza-Paleopalinoteca-Laboratorio-Paleopalinología) at IANIGLA. England Finder coordinates are given for the illustrated specimens.

The fossil invertebrates were collected during several field trips to the Cerro Bandera locality (2002, 2006, and 2009), from tuffite and shale levels The samples have been catalogued in the Palaeoinvertebrates Collection (MPEF-PI) of the Museo Paleontológico Egidio Feruglio in Trelew, Chubut province, and also in the Palaeozoological Collection (CTES-PZ) at the Universidad Nacional del Nordeste and the Centro de Ecología Aplicada del Litoral (CECOAL). These samples were examined using an Olympus SZ51 stereoscopic microscope as well as using the scanning electron microscope at the Universidad de Buenos Aires.

4. Sedimentology

4.1. Facies associations (Table 1)

4.1.1. Lacustrine limestones (SIP, OW, MM, and OL; Fig. 2)

Sandy intraclastic packstone (SIP; Figs. 2, 4a): This facies is represented by tabular beds (1–1.20 m thick) which run laterally for about 20 m. These beds present ripple cross-lamination made up of cosets (10 cm thick), with predominantly thin (1 to 2 cm) undulating lamination. Grain size is variable (fine–medium), clasts are angular to sub-rounded and well-sorted. Siliciclastic grains (25%) are present as quartz and feldspar crystals, along with lithic fragments (basalt, andesite, metamorphic rock, and pyroclastic materials). Intraclasts (20%) are composed of micrite and microspar. Bioclasts (3%) are mainly fragmented and reworked ostracod shells measuring around 400 μm on the long axis, fish scales (60 μm) and algal remains (250 μm). The cementing material is silica (chalcedony or quartz), and it infills the cavities. These are elongated, with irregular shapes, and in general with no preferential orientation in the microfacies. Their average dimensions are 43 μm long by 6 μm wide. The matrix has been recrystallized to spar, presenting crystals of dolomite with xenotopic texture, which form a homogeneous mosaic where the crystals are anhedrals with irregular intercrystalline boundaries (Gregg and Sibley, 1984). Thin layers (~4 cm thick) formed by prismatic gypsum crystals (3 mm) have been identified at different bearings within the facies.

Interpretation: This facies is interpreted as representing littoral lacustrine depositional areas near the inflow point of detrital fluvial sediments, which were sourced from more elevated surrounding areas. The tabular shape of the beds along with the type of stratification (ripple cross) indicates sedimentation in shallow bodies of water, with oscillatory flow (Morsilli and Pomar, 2012) that produced wave movement. Silicification resulted from pre-existing quartz-rich sediments. The silica has been removed by deep weathering processes under highly acidic conditions, and then infilled the pores and voids found in the original sediments when conditions changed (Rabassa, 2010). Lacustrine gypsum layers indicate an intermediate to marginal lake zone (Orti et al., 2003).

Ostracod wackestone (OW) (Figs. 2, 4b): This facies overlies the SIP facies aforementioned. It is 1.50 m thick in 0.20 m beds, with symmetrical

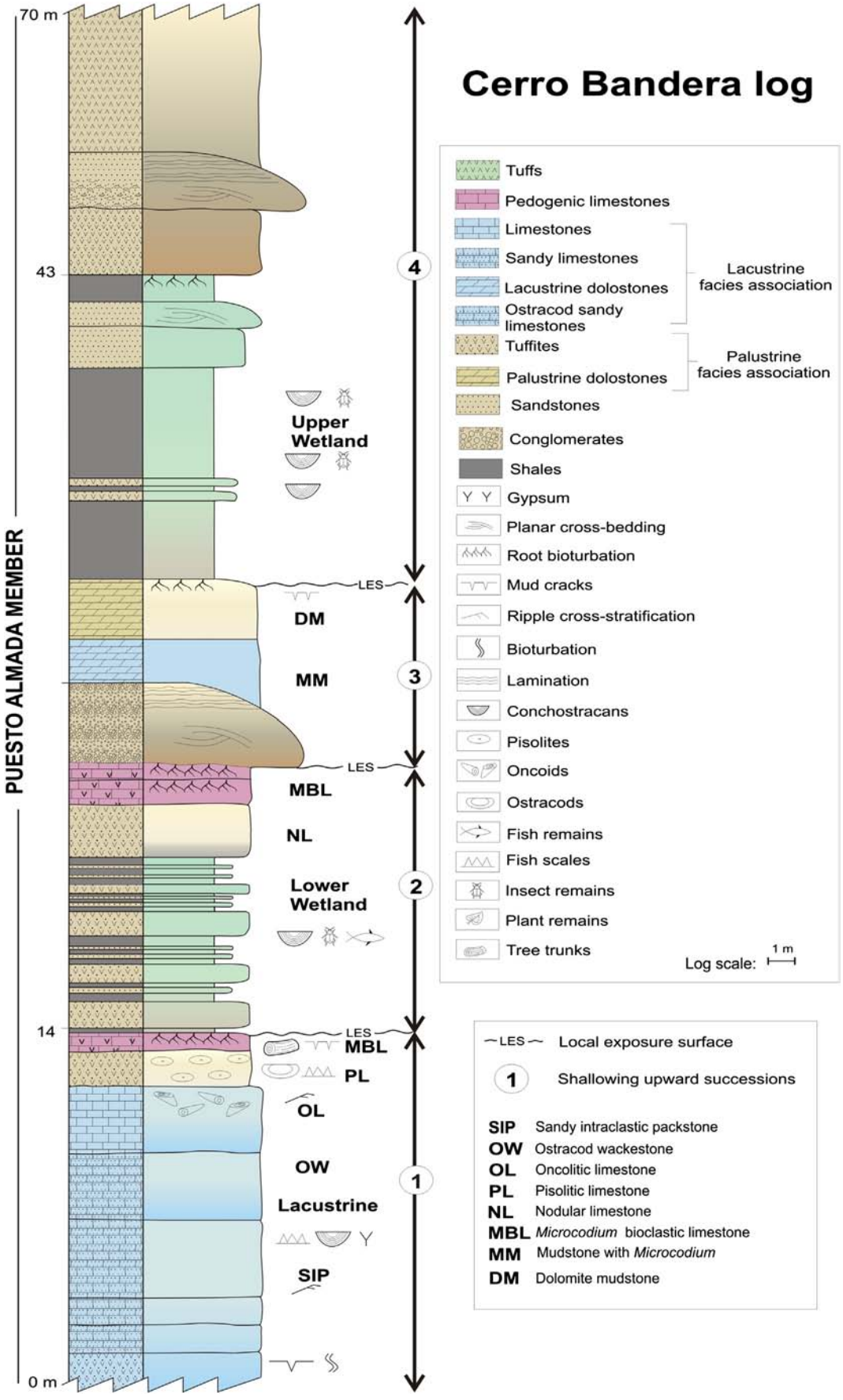

Fig. 2. Stratigraphic log of the Cerro Bandera locality in the Fossati sub-basin (Cañadón Asfalto Basin).

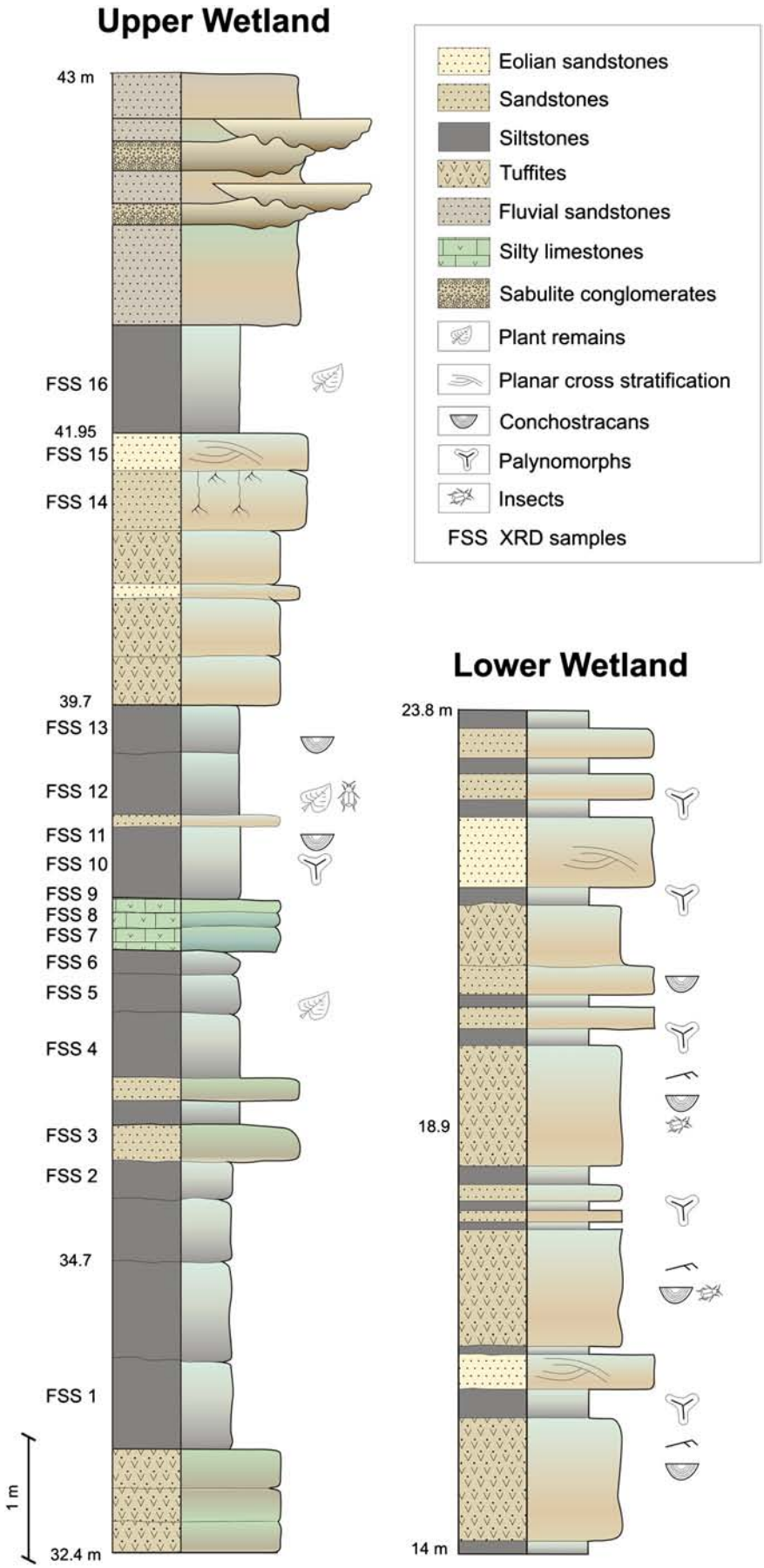

Fig. 3. Detailed profiles of the wetland sedimentary levels of Fig. 2, at the Cerro Bandera locality in the Fossati sub-basin (Cañadón Asfalto Basin).

Table 1
Summary of facies associations from the Puesto Almada Member at Cerro Bandera locality and their sedimentological and palaeoenvironmental characteristics.

Facies associations	Facies/Microfacies	Lithology	Structures	Bedding	Fossil content	Lateral and vertical relationships	Interpretation
Lacustrine limestones	Sandy intraclastic-packstone (SIP)	Well-sorted limestones, angular to sub-rounded siliciclasts	Ripple cross stratification	Tabular beds 1–1.20 m thick, 20 m long	Ostracod shells, fish scales and algae remains	Vertical variation of OW	Littoral subenvironment
	Ostracod wackstone (OW)	Micrite limestone	Symmetric ripple cross stratification	Beds 1.50 m thick in sets of 0.20 m	Aligned ostracod shells, conchostracan shells and marks of insect	Vertical variation of SIP	Ponds affected by wave action
	Mudstone with Microcodium (MM)	Micritic limestone	Disrupted fabric	Tabular beds 2 m thick	Conchostracan, disarticulated ostracod shells	Vertical variation of DM, lateral variation of the Alluvial fan facies association	Margins of shallow lake and vadose subenvironments
	Oncolitic limestone (OL)	Limestone	Oncolitic fabric	Lenticular beds 60 cm thick and 8 m of lateral extent	Plant debris and ostracod valves	Vertical variation of OW and PL, lateral variation of OW	Carbonate ponds related to palustrine setting
Palustrine limestones	Dolomite mudstone (DM)	Dolomitic limestone	Without internal structure and homogeneous in composition	Beds 2 m thick	Ostracod shells	Vertical variation of MM	Palustrine subenvironment affected by pedogenesis
	Pisolite limestone (PL)	Limestone	Pisolithic	Tabular beds 8 m long and 0.80 m thick	Ostracods and fish scales	Vetical variation of MBL and OL, lateral variation of MBL	Vadose–phreatic zone of palustrine subenvironment
	Nodular limestone (NL)	Limestone	Brecciation	Tabular bed of 1.60 m		Vertical variation of the Claystones and siltstones	Vadose zone of palustrine subenvironment
	Microcodium bioclastic limestone (MBL)	Limestone	Disrupted, brecciation	Tabular bed 8 m long and 1.20 m thick	Microcodium algae and ostracods	Overlies PL, related with Claystones and siltstones	Pedogenic subenvironment with paleosol development
Pyroclastic deposits	Pyroclastic limestones, siltstones and sandstones	Tuffitic carbonates, sandstones, siltstones and tuffites	Massive	Tabular and lenticular beds of several tens of metres	Root and metazoan bioturbation	Vertical variations of Palustrine limestones and Claystones and siltstones	Fall deposits in the lacustrine–palustrine subsettings
Aeloian deposits	Yellowish white sandstones	Medium-coarse, well/ very well-sorted	High angle trough cross stratification	Tabular beds up to 25 m long and 2 m thick	Metazoan burrows	Interbedded with the Palustrine limestones, Claystones and siltstones	Aeolian deposits associated to wetlands
Aluvial fan and fluvial deposits	Reddish green sandstones	Medium-coarse, well/ very well-sorted	High angle trough cross stratification	Lenticular beds 20 m long and 0.2–20 m thick	Metazoan burrows	Overlies the Claystones and siltstones, laterally interbedded with the Lacustrine limestones	Fluvial channels associated with the distal alluvial fan
	Matrix-supported conglomerates	Immature texture, angular to rounded clasts, granule to boulder of andesite, basalt, chert, tuff, and migmatite, poorly/ very poorly sorted	Planar cross stratification	Coalescent lobular beds 3 m thick and 80 m long in units of 5 km in lateral extent	–	Capping the Claystones and siltstones	Distal alluvial fan
	Green sandstones	Immature to mature texture, lithic arenite, sublithic arenite, and quartz arenite	Planar cross stratification	Lenticular	–	Capping the Claystones and siltstones	Streams of fluvial systems associated with the distal alluvial fan
	Red tuffitic sandstones	Siliciclastic feldspar (orthoclase) and quartz, medium to coarse, moderately/ poorly sorted	Planar cross stratification	Lenticular beds 20 m long and 0.2-20 m thick	–	Capping the Claystones and siltstones	Bars of fluvial systems associated with the distal alluvial fan
Claystones and siltstone deposits	Claystones and siltstones	Black to brownish grey shales and claystones, predominantly analcime	Massive	Tabular, 0.80 m thick, lateral extent 5 to 8 m	Conchostracans, caddisfly cases, carbonaceous plant remains, and preserved OM	Overlies DM and MBL, laterally interbedded with Pyroclastic deposits	Alkaline-brackish wetlands

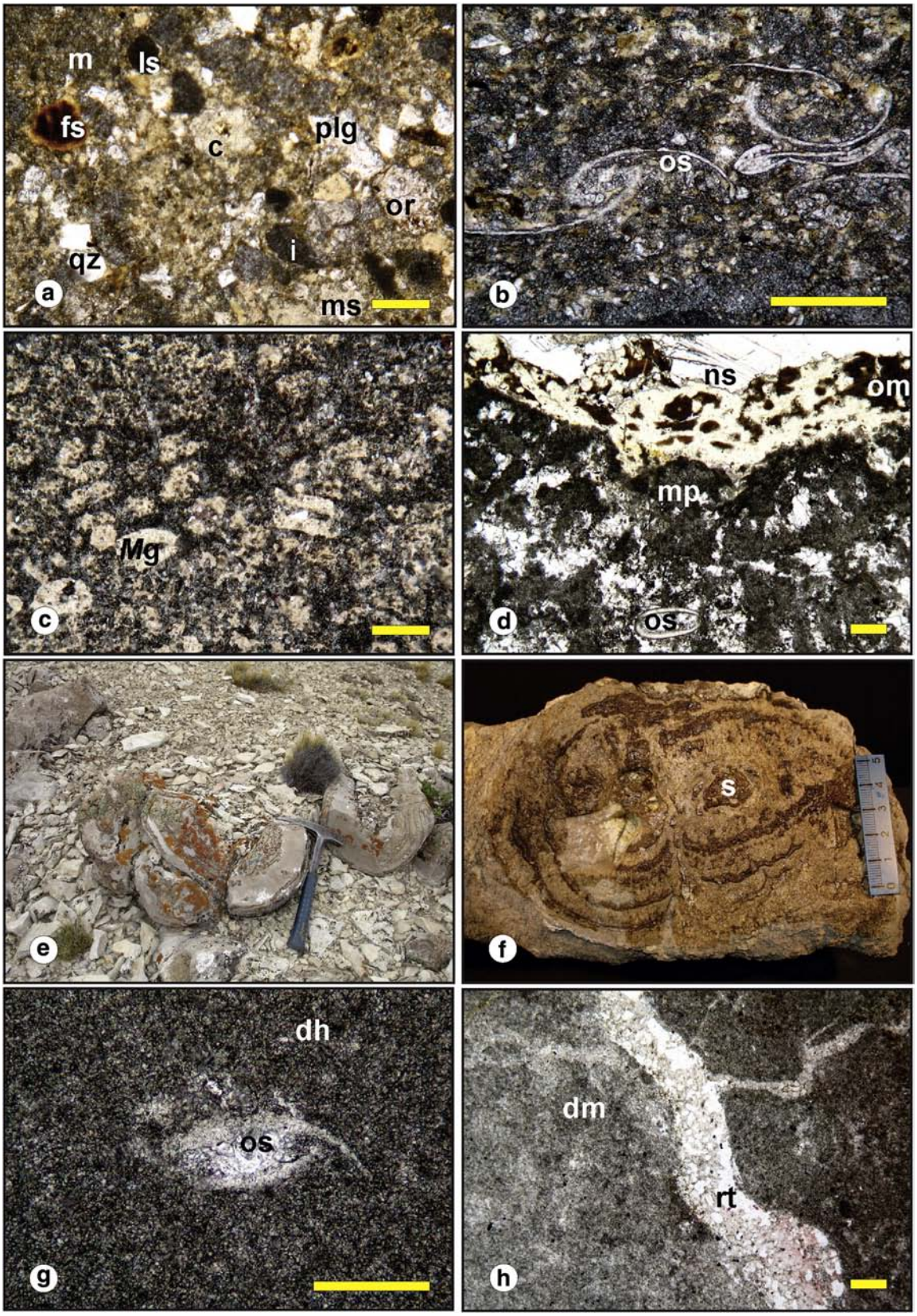

Fig. 4. Thin section photographs of microfacies SIP, OW, NW, DM, OL, Puesto Almada Member, Cañadón Asfalto Formation (Jurassic). a SIP, microfacies showing quartz (qz), orthoclase (or) and plagioclase (plg) siliciclasts, lithics (ls) and intraclasts (i), bioclasts represented by fish scales (fs). Matrix is micrite (m), the cavities are filled by chalcedony (c) and microcrystalline silica (ms); b OW, microfacies where aligned ostracods shells (os) can be seen immerse in a micrite matrix replaced by microspar; c MM, *Microcodium* grain (*Mg*) transverse and longitudinal sections included in the thin layers of the microfacies; d OL, concentric oncoid showing nucleous of silica (ns) and organic matter (om), an articulate ostracod shell (os) is in micrite pendant vadose cement (mp); e outcrops of giant oncoids showing concentric lamination and mould of organic infilling of the nucleous; f transverse section of giant oncoid with thick, crenulated concentric lamination of the micrite and silica, nuclei of the sparite (s); g DM, dolomite mudstone with matrix composed of dolomite forming a homogeneous mosaic (dh), the bioclast is an ostracod (os) with articulated valves; h DM, detail of root trace (rt) in dolomitic matrix (dm). Scale bars = 3 mm.

ripple cross stratification. Bioclasts (10%) are mainly aligned ostracod shells 60 μm long and 30 μm in transverse section, and a minor amount of 'conchostracan' shells (100 μm). Rare fragments of *Microcodium* are scattered in the matrix. Circular structures recrystallized to pseudospar have also been identified. These measure 20 μm in diameter in the transverse section and 60 μm in the longitudinal section, and they have a micritic wall. Intraclasts (5%) are angular micrite and have an iron oxide coating. Clastic grains (3%) are only rarely covered with iron oxides and are represented by quartz, orthoclase and plagioclase crystals, along with other metamorphic and igneous grains. The elongated pores (2 mm long by 40 μm wide) are isolated and are parallel to the stratification plane. The micropores (4 μm of diameter) are irregular and interconnected. Pores are filled with dolomite, and larger cavities with microcrystalline silica and quartz. Elongated and irregular horizontal sedimentary structures (cracks) of approximately 2.36 mm long and 600 μm wide disrupt the matrix, they are filled by spar and have micrite walls (100 μm).

Interpretation: First, the disposition of the bioclasts indicates a marginal setting within ponds in which oscillatory wave movement resulted in shell alignment. Secondly, *Microcodium* grains suggest the presence of calcified roots associated with calcareous soils and carbonate substrates (Freytet and Plaziat, 1982; Jaillard et al., 1991; Wright, 1994; Arp, 1995; Košir, 2004). The presence of cavities is interpreted as bioturbation probably related to metazoan infaunal activity (Bromley, 1996; Buatois and Mángano, 1998). Moreover, scarce circular structures have been identified as 'conchostracans' eggs. All these features imply a palustrine subsetting (Alonso-Zarza et al., 1992) associated to the ponds margins. The presence of an iron mineral cover on the intraclasts indicates that most likely there were changes in the groundwater redox potential related to fluctuations in the phreatic level (Freytet and Plaziat, 1982).

Mudstone with *Microcodium* (MM) (Figs. 2, 4c): This facies forms tabular beds 2 m thick with a broad areal distribution (80 m long). *Microcodium* is present either as individual dispersed prisms (5%) or rarely as prism groups (1%). It mainly forms thin layers (2 mm thick) with the long axis of the prisms oriented parallel to the stratification surface. Transverse sections measure 140 μm in diameter on average, and the longitudinal sections are about 180 μm wide by 280 μm long. Invertebrates are represented by remains of the 'conchostracan' *Congestheriella rauhuti* (Gallego et al., 2010). The matrix is mainly peloidal micrite with detrital contribution, disrupted by vertical structures about 4 μm wide and 0.4 mm long. These disruptive structures are replaced mainly by opal silica and scattered dolomite crystals. *Microcodium* and cavities are replaced by silica (isotropic opal, Type II, Bustillo and Alonso-Zarza, 2007), and partially by dolomite. Dolomite crystals show different distribution patterns in the matrix: a) as thin lamina (20 μm); b) as homogeneous mosaics of equi-granular crystals (1 to 3 μm); c) as aggregates associated with opal (40 μm); and d) as individual, dispersed clear crystals lacking inner structure (80 μm). The crystals in this facies also present different morphologies: rhombohedral, and anhedral. Calcite has been identified as pendant cement associated with *Microcodium* algae and 'conchostracan' shells.

Interptetation: Our interpretation is that the limestones in this facies formed in the marginal zone of shallow lakes where macrophytes were present, whilst the presence of 'conchostracans' indicates subaqueous deposition. The *Microcodium* was probably transported from pedogenic environments (Košir, 2004). Individual prisms, disaggregated and orientated, are interpreted as reworked intra-basinal particles coming from other areas of the basin where palaeosols developed (Arribas et al., 1996). The silicification and dolomitization are interpreted as resulting from vadose environmental diagenesis, whilst dolomitization has also affected the previously silicified deposit because of meteoric phreatic level fluctuations (Bustillo and Alonso-Zarza, 2007).

Oncolitic limestone (OL) (Figs. 2, 4d). These layers extend approximately 8 m laterally and are 60 cm thick, they occur as lenticular-shaped bodies, which pinch out at both ends. This facies contains abundant coated grains, mostly giant oncoids (Fig. 4e–f), that range in size from 20 to 60 cm in diameter. The nuclei of the oncoids are commonly composed of phytoclasts such as macrophyte plant stems. The oncoids show concentric micrite laminae and micropeloids. The facies has a fenestral fabric that is composed of cavities filled with spar or rarely with fibrous-radial quartz. Ostracod shells can also be found in these cavities. The cement infilling the cavities is pendant micrite and meniscus.

Interpretation: The geometry of the strata suggests that this facies represents the marginal zone of a carbonate pond that developed in a larger palustrine setting. The presence of coated grains of microbial origin provides evidence for waters with carbonate content and containing cyanobacteria-like algae. These two elements, one inorganic (the carbonate source) and the other organic, triggered carbonate precipitation in the pond (Shiraishi et al., 2008). The submerged parts of these plants became calcified and were coated by microbial biofilms. The pendant and meniscus type of cements are indicators of a vadose setting. Similar palaeoenvironments have been proposed by other authors (Arenas et al., 2007; Arenas-Abad et al., 2010; Benavente et al., 2012) for similar facies containing oncoids and for phytoclast facies.

4.1.2. Palustrine limestones (DM, PL, MBL, and NL; Fig. 2)

Dolomite mudstone (DM; Figs. 2, 4g–h): This facies is about 2 m thick. The matrix is constituted by peloids that are mostly spherical in shape (20–40 μm in diameter), and partly agglutinated, along with dolomite that forms a homogeneous mosaic with rhomboid, anhedral and rounded crystals over 1 μm in diameter. Bioclasts (1%) consist of disarticulated ostracod shells (about 40 μm). Thin, irregular vertical sedimentary structures (3 cm long and 200 μm wide) are filled with fibrous-radial spar and microcrystalline quartz. These structures have smooth, rounded margins, and show distinctive helicoidal patterns in the microfabric. Also present are cavities not exceeding 2 cm long and 600 μm wide, with discontinuous micritic walls (80 μm), and associated with cutans. These are predominantly filled by very fine size quartz (average 110 μm), orthoclase, plagioclase and carbonate, and are partially recrystallized by dolomite (4 μm crystals), spar, and fibro-radial quartz and microcrystalline silica.

Interpretation: The cavities with cutans are interpreted as rhizobrecciation, and two different stages of intergrowth and pedogenesis are observed (*sensu* Freytet and Plaziat, 1982). The first stage corresponds to dolomite and spar replacement and the second to the different varieties of silica. Fibrous-radial and microgranular quartz may have resulted from silica precipitation in organic matter associated with microbial films (Knoll, 1985; Sanz-Montero et al., 2008). In this particular case, the precipitation could be associated with organic matter decay in the rhizosphere environment, where microorganisms are abundant as well. The thin, irregular vertical cavities are interpreted as bioturbation by infaunal metazoans (Freyt et al., 1984; Buatois and Mángano, 1998; Hasiotis et al., 2006), based upon the lack of cutans, morphological features (walls, sizes), and their distribution pattern in the microfabric. The features described belong to palustrine environments affected by pedogenic processes.

Pisolitic limestone (PL; Figs. 2, 5a–c): The facies occur as tabular beds, 8 m long and 0.80 m thick, formed by pisolites up to 3 cm diameter with diffuse concentric lamination, defined by a concentration of carbonate particles, intraclasts, and siliciclasts. Tree trunk remains up to 30 cm long are also present in this facies, which is formed by a micrite and silica intraclast packstone (25%). Angular to well-rounded siliciclastic grains (3%) correspond to quartz and feldspar, and igneous and metamorphic lithic fragments are also present. The bioclasts present are ostracods (approximately 40 μm in transverse section) and fish scales (10 μm). The matrix is micrite, and pores have been infilled by fibrous-radial silica, microcrystalline silica, spar, and granular dolomite. Intraclasts have been replaced by microcrystalline silica.

Interpretation: The pisolites are linked to a vadose freshwater environment since they lack a skeletal nucleus and encrusting biota. This environment is likely in a palustrine setting with pedogenic influences

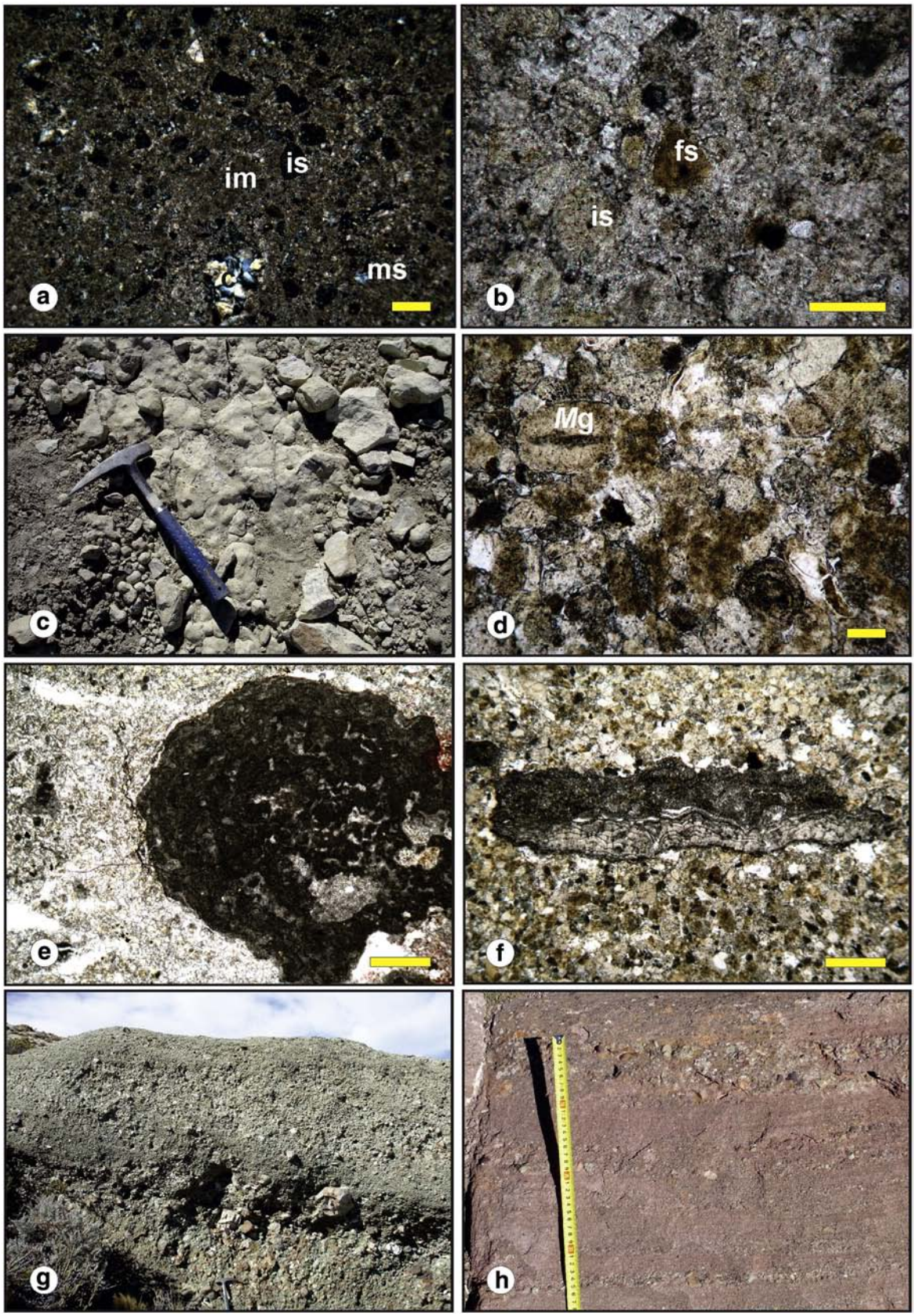

Fig. 5. Microfacies and outcrops photographs of the Puesto Almada Member (Upper Jurassic) in the Cerro Bandera locality, Cañadón Asfalto Basin. a PL, intraclasts of silica (is) and micrite (im), siliciclasts grains of quartz, orthoclase, plagioclase and igneous and metamorphic rocks, pores infilled by chalcedony (c) and microcrystalline silica (ms); b PL, detail of fish scale (fs) and intraclasts recrystallized to microcrystalline silica (is); c plain view of the PL facies; d MBL, longitudinal sections of *Microcodium* grains (*Mg*); e MBL, detail of fragmented microbialitic intraclast; f NL, discontinuous laminar micritic intraclasts with mud cracks; g clast-supported conglomerate. The conglomerate levels have lobular geometry with internal cross-bedding, and present erosive bases above a coarse sandstone level. Plant for scale = 1 m high; h red sandstones with planar cross stratification and conglomeratic interbeddings. Scale bars: a,b,d = 1 mm; e,f = 5 mm.

(Armenteros et al., 1997). The concentric pisolitic structures can be associated with pedogenic influence, root activity, or related to rounded siliciclastic or carbonate particles (Flügel, 2004). The silicification observed is attributed to diagenesis in the vadose/phreatic zone of a palustrine environment (Bustillo and Alonso-Zarza, 2007).

Microcodium bioclastic limestone (MBL; Figs. 2, 5d–e): This facies corresponds to a 1.20 m thick layer overlying the Pisolitic limestone (PAF6). It is made up of intraclasts (25%) of microcrystalline silica (17%) and micrite (8%). The micrite intraclasts are microbialite fragments of 4 mm long and 1 mm wide, horizontally disposed. They show homogeneous and flat laminated micrite associated with pyrite. These fragments are associated with cracks of 2 cm long and 16 μm wide that disrupt the fabric and are filled with calcite and opal. Also scarce oncoids (5%) are recognized in the facies matrix, they present 20 μm in diameter with a siliceous, sparitic or micritic core. *Microcodium* (44%) is represented in the facies matrix mainly by individual grains of 20 μm and bioclasts are scarce, disarticulated ostracod shells, also of approximately 20 μm. Siliciclastic grains (<1%) are scarce and correspond to highly altered lithics or quartz. Chalcedony is observed infilling vugs and replacing intraclasts, and microgranular dolomite was also observed in some areas.

Interpretation: The dominance of *Microcodium* in the facies indicates rhizosphere development (palaeosols) (Košir, 2004). The mud cracks are interpreted as having been formed by root bioturbation (Freytet and Plaziat, 1982). These features support an interpretation of deposition in a pedogenic environment (Freytet and Plaziat, 1982; Alonso-Zarza and Wright, 2010). The microbialitic intraclasts probably resulted from disruption of an original microbial mat by later pedogenic processes (Arenas et al., 2007; Busquets et al., 2007).

Nodular limestone (NL; Figs. 2, 5f): This facies forms a 1.60 m tabular layer with brecciation of the original carbonate sediments. Two types of intraclast (30%) were recognized: a) discontinuous laminar limestone with micrite, microspar, and spar nodules, with mud cracks filled with silica; and b) micrite–dolomite with mud cracks filled with granular sparite. The micrite has been recrystallized to crystalline dolomite and opal. Spar and microspar are present as pendant cement.

Interpretation: The intraclasts observed in this facies were formed under subaqueous conditions but have pedogenic alteration features (mud cracks, brecciation) (Freytet and Plaziat, 1982; Alonso–Zarza and Wright, 2010). These secondary features and the presence of pendant cements suggest late deposition of the intraclasts in a vadose setting (Alonso-Zarza and Arenas, 2004).

4.1.3. Alluvial fan matrix-supported conglomerates and fluvial sandstones

Matrix-supported conglomerates (Figs. 2, 5g): The conglomerate strata present lobule shape with erosive bases and internal erosive surfaces. They are very thick (3 m) and have an extensive lateral distribution (80 m). They are characterized also by green colour and an immature texture. Clasts sizes range from granule to boulder, with size sorting being poor to very poor. They are angular to rounded, and composed of andesite, basalt, chert, tuff, and migmatite. The conglomerates present normal grading and planar cross stratification. They are interbedded with very fine granules and very thick matrix-supported green sandstones.

Interpretation: The lobate geometry of these deposits, their lateral coalescence as well as their lithological and sedimentological characteristics, indicate the input of a variety of lithic materials from sloping areas of the basin associated with alluvial fans. A transition from gravel to graded sands towards the marginal areas of alluvial fans represents a shift to mixed-load dominant deposition (Dunagan and Turner, 2004; Turner and Peterson, 2004). The alluvial fan deposits are related to ephemeral lacustrine deposits, and were formed over the marginal lacustrine subenvironment.

Red and green sandstones (Fig. 2): Red sandstones (Fig, 5 h) are interbedded with thin layers (20 cm) of conglomerates, silty tuffites and mudstones. These sandstones form tabular to lenticular beds of several tens of metres long and 2 m thick, with an erosive base. The clasts are basalts, limestones, cherts, migmatites, tuffs, and tuffites; poorly/moderately sorted, and they lack any preferred orientation. The strata present a vertical coarsening upwards trend, and sometimes they present planar stratification.

Green sandstones (Fig. 6a) show planar cross stratification, and the coset thickness is 10 cm. These layers include compositionally and texturally immature to mature lithic arenite, sublithic arenite, and quartz arenite sandstones (Folk et al., 1970). Grains are mainly igneous (andesites and basalts) and sedimentary (chert, limestones, and sandstones). In the lower proportion metamorphic grains (migmatites) and feldspars (<25%) and quartz (<5%) are identified. Framework grains range from coarse silt to very coarse sand, angular to well-rounded, and very poorly to very well-sorted.

Red tuffitic-sandstone deposits form lenticular beds 20 m long and 0.2–20 m thick that overlie the silty tuffites. These layers present planar cross stratification and are related to sabulous lenses, siliclastic grains are feldspar (orthoclase) and quartz. Grain size is medium to coarse, with moderate/poor sorting.

Interpretation: The green sandstones are interpreted as channel deposits related to alluvial fans. The red sandstones are interpreted as bar deposits in braided channels (Miall, 1996; Sánchez et al., 2005). The textural maturity indicates a reduced relief for the source area and enlargement of the catchment basin near the source area.

Claystones and siltstones (Figs. 2, 6b): This facies is represented by black to brownish grey shales and claystones in beds of 0.80 m thick or less, and wide lateral extent (5 to 8 m). These are interbedded with layers up to 0.40 m thick of silty tuffites, and thin levels (8 cm) of massive fine sandstones. The siltstones contain 'conchostracans', caddisfly cases, disseminated carbonaceous plant remains, and preserved organic matter (OM). Also, the presence of minor features that disrupt the fabric, as cracks and voids, are observed but the beds are generally massive. The claystones and siltstones are mainly composed of quartz, feldspars (plagioclase and/or K-feldspar), and clay minerals, although subordinate calcite also occurs in a few cases (Table 2). Analcime was identified in varying amounts in most of the bulk rock samples, as well as the less than 2 μm sub-fraction. The clay mineral assemblages identified by XRD are dominated by smectite, with subordinate mica and less frequently kaolinite, and with chlorite and mixed-layers (illite/smectite or corrensite) occurring in subordinate amounts or absent (Table 2).

Interpretation: The massive fabric of the strata and their minor disruption suggest deposition in marshes and wetland areas during pond-expansion episodes, with incipient palaeosol development and exposure. The major depositional mechanism was suspension of the fine sediment. These massive levels are formed by detrital material within a micrite matrix with abundant clays and which occasionally develop crumbs. Siliciclasts are grains of quartz, feldspar, basement migmatites, chalcedony, sandstone, and limestone. The preservation of OM and plant remains indicates at least disoxic conditions in the environment.

The widespread occurrence of analcime in the wetland sediments suggests persistently alkaline-brackish water (Boles and Surdam, 1979). The origin of the analcime is uncertain, it could have formed directly from volcanic glass or by replacement of a primary zeolite, since clinoptilolite/heulandite was identified (with uncertainty) in only one of the levels studied. It is likely that the smectite dominating the clay assemblages, was formed by authigenesis (via early diagenesis) from highly labile volcaniclastic material (Cuadros et al., 1999) sourced from the abundant tuff beds of the succession. Further support for this interpretation is the low fluvial clastic input that characterizes the wetland environments. The scarcity of kaolinite reflects low analcime abundance that probably is detrital in origin. This is because this mineral is formed in acidic environments associated with SiO_2, and should consequently be highly unstable in an alkali medium. According to stability diagrams, in solutions that are saturated with respect to amorphous silica, and under standard pressure and temperature conditions, kaolinite

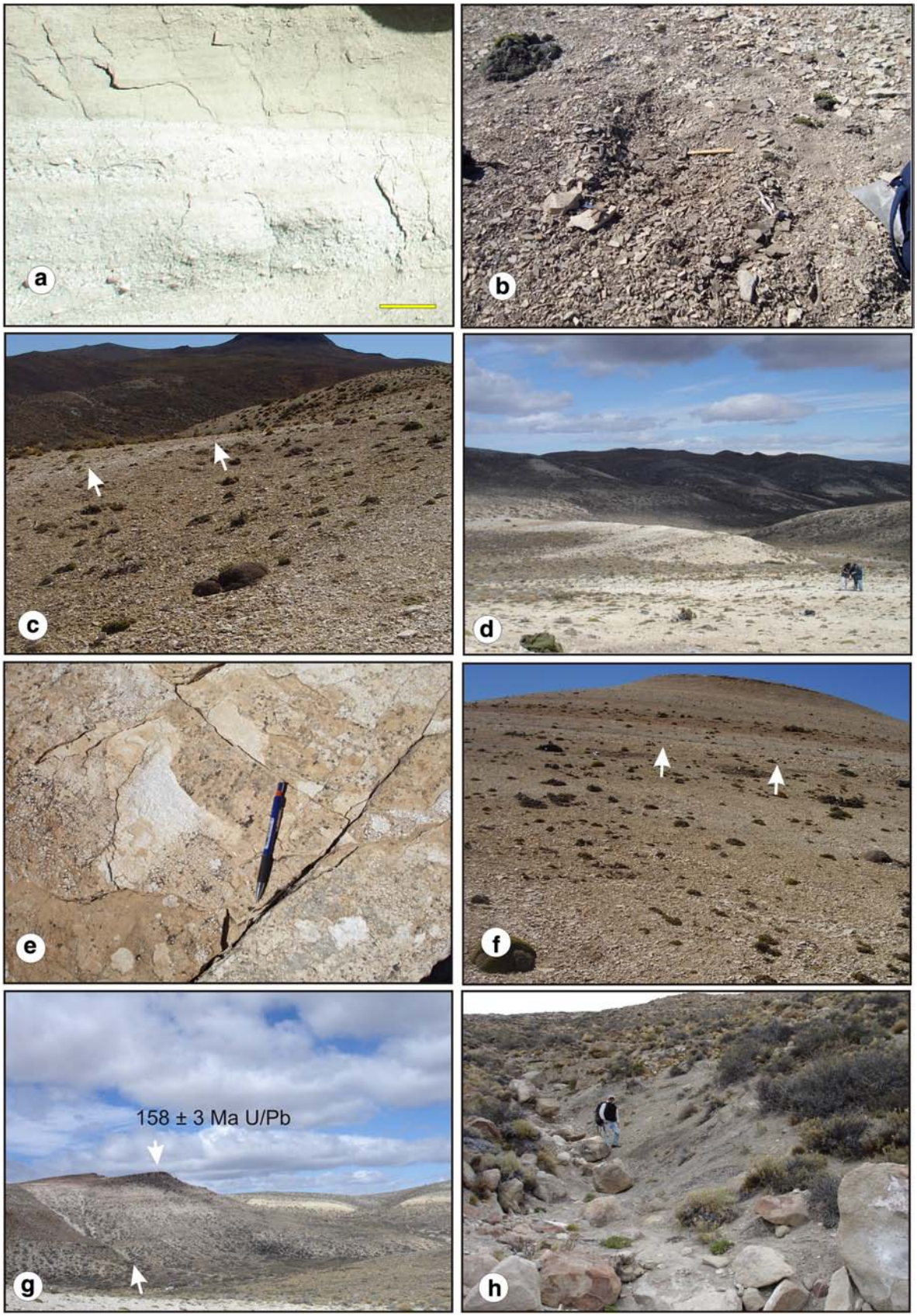

Fig. 6. Field photographs of the Puesto Almada Member (Upper Jurassic) outcrops at the Cerro Bandera locality, Fossati sub-basin, Cañadón Asfalto Basin, a green sandstones showing planar cross stratification and cut and fill structures. Scale = 10 cm; b siltstone facies where the palynomorphs and palaeoinvertebrates were obtained from; c white eolian sandstones (arrows) interbedded with siltstones of the wetland; d people standing over the pyroclastic material interbedded with siltstones of the wetland subenvironment and sandstones; e silty tuffites level showing mud cracks, interbedded with fluvial sandstones of the upper succession; f general view of the lower wetland deposits; g detail of the section where the log was done (upper wetland) (arrow); h detail of g, exactly where the log was done, OFG for scale.

Table 2
XRD results from the upper wetland claystones and siltstones. MIL: mixed-layered clay minerals; I/S: mixed illite-smectite -layers; Sm: smectite; Chl: chlorite; Kln: kaolinite; X: presence.

Samples	Clay Mineralogy								
	Sm	Micas	Kln	Chl	ML	Anl	Qz	Kfs	Plg
FSS1	X	X		?		X	X		X
FSS2	X	X	?	?		X	X	X	
FSS3	X	X				X	X	X	X
FSS4	X	X		?		X	X	X	X
FSS5	X	X		?		X	X	X	X
FSS6	X	X		?		X	X	X	X
FSS7	X	?	?	?		X	X	X	X
FSS8	X	?			I/S?	X	X	X	X
FSS9	X	?			I/S?		X	X	
FSS10	X	?	X	?	I/S?				
FSS11	X		X		Crr?	?	X	X	X
FSS12	X	?			I/S?		X	X	
FSS13	X		X		I/S	X	X	X	
FSS14	X			?		X	X	X	X
FSS15	X				I/S?	X	X		X
FSS16	X		X	?		X	X	X	X
4/12/07-1	X				I/S	X	X		X
24/03/09-3	X						X	X	X
CCDM-1	X						X		

is stable in environments in which log $[K^+]/[H^+]$ and log $[Na^+]/[H^+]$ are lower than ~13, whereas with an increase in Na^+ and K^+ activities in relation to $[H^+]$, kaolinite becomes unstable and montmorillonite (smectite) becomes the stable phyllosilicate (Faure, 1998) instead. Therefore, an assemblage with smectite + analcime ± calcite is consistent with a pattern of predominantly volcaniclastic inputs into the wetland and only scarce fluvial clastic input in an overall arid climate context. On the other hand, the kaolinite-bearing layers would correspond to wetter climatic periods, with a relatively higher level of fluvial input, which would also lead to decreased alkalinity and salinity for wetland waters.

4.1.4. Aeolian sandstones

White sandstones (Figs. 2, 6c): Bright yellowish white sandstones form tabular beds up to 25 m long and does not exceed 2 m thick constituting a thin unique intervening section in the succession. The beds show high angle and trough cross stratification. Siliciclastic grains are quartz and feldspar (orthoclase), and pyroclastic material, medium to fine in size, and well/very well-sorted.

Interpretation: The characteristics of the deposits (scarce extent, stratal geometry, sedimentary structures, composition, and sorting) and their position overlying the fluvial plain sandstones adjacent to channel deposits, have affinities with aeolian deposits overlaying the wetlands succession as a thin unique record. Given the limited extent of these beds not much more data can be provided. Most likely the sediments were carried by the prevailing SW winds from higher terrains and filled lower lying areas, thereby indicating the probable dryness in the basin.

4.1.5. Pyroclastic deposits

The pyroclastic deposits (Fig. 6d) consist of tuffs and tuffites interbedded with limestones, volcanic silt layers with mud cracks (Fig. 6e), sandstones and conglomerates. Tuffites are mainly volcanic mudstone with crystaloclasts and few shards (tuffaceous lime). They are formed by a very fine laminated matrix composed of volcanic dust, which contains iron oxides and organic matter. Shards are generally rare and no larger than 100 μm. Their content is varied, fine, and includes fine vesicular glass, cuspade, and worn pumicite fragments. Volcanic crystaloclasts are composed of quartz. Bioclasts (4%) are represented by 'conchostracans', ostracod shells, and isolated caddisfly cases. There is evidence of devitrified glass and alteration of clays. Tuffs are yellowish brown and have thin and fine discontinuous black pumiceous levels. The microstructure is complex, with a lamination produced by the differences in argillaceous material contents. The groundmass is homogeneous, made up of glass with fluidal structure and aligned microgranules of clay.

Interpretation: The tuffites, that show a low degree of welding, indicate pyroclastic fall deposits in lacustrine environments. The tuffite deposits present scattered fractures, which occur when very hot volcanic material falls directly into water, thereby producing fast cooling (Koukharsky et al., 2002).

4.2. Stacking pattern

The succession studied presents an aggradational stacking pattern with four shallowing upwards successions defined by local exposure surfaces, which represent different palaeoenvironments. The first shallowing upwards succession is formed by the Lacustrine facies association that is overlain by the gradual transition to the Palustrine facies association ending with a pedogenic facies associated with an exposure surface (0 to 14 m; Fig. 2). These facies represent an environmental evolutionary sequence from lacustrine, to palustrine, to pedogenic subenvironments. This section is also characterized by the association of 'conchostracan' (*Congestheriella rauhuti*) and ostracods (*Penthesilenula sarytirmenensis* and *Theryosinoecum barrancalensis minor*) populations. Demko et al. (2004) have reported similar palaeosols development at the top of aggradational successions in the Morrison Formation from the Upper Jurassic of the United States of America where palaeosols were formed in marginal lake environments and also on floodplains.

The second succession is made up of a Palustrine facies association that represents sedimentation in a wetland subenvironment (14 to 24 m; Figs. 2–3, 6f), which is also capped by a pedogenic facies. The palaeontological assemblages consists of 'conchostracans' (Euestheriidae), ichnofossils (caddisfly cases), insects, fish scales, and palynoflora remains.

The third succession (24 to 30.5 m; Fig. 2) shows a trend towards progradation, represented by the coarse sediments of the Alluvial fan facies association (see 4.1.3.), indicating clastic inputs into the basin and again a drop in the lake level. Towards the top of the succession a rise in the lake level is indicated by the Lacustrine facies association overlaying the Alluvial fan facies association.

The fourth succession is represented by a second wetland episode (30.5 to 70 m; Figs. 2–3, 6g–h) similar to the previous one and also capped by a coarse clastic input layer. Its fossil content include 'conchostracans' (Palaeolimnadiopseidae), ichnofossils (caddisfly cases), and a palynologic assemblage. It is worth noting that in this succession the beds containing 'conchostracans', as well as the ones yielding plant remains are those also showing low levels or no levels of analcime, and subordinate kaolinite. As kaolinite is formed in an acidic environment associated with SiO_2 and is highly unstable in an alkali medium, its occurrence indicates less alkaline/saline conditions than those in the beds dominated by smectite, which according to stability diagrams becomes a stable phyllosilicate with increased Na^+ and K^+ activity in relation to $[H^+]$ (Faure, 1998). These lower analcime abundances in kaolinite-bearing levels constitute further evidence for lower alkalinity/salinity.

5. Palaeontology

5.1. Palynology

The samples yielding the palynomorph assemblages were extracted from deposits of the wetland subenvironments (successions 2 and 4; Figs. 2, 3). They comprise layers of brownish grey tuffaceous claystones, black claystones with organic matter, and black shales, interbedded with tuffites and sandstones. The species recorded in this study provide information on the environment of deposition but do not allow for

precise age dating of the Puesto Almada Member as they have a wide Jurassic–Cretaceous biochron.

For the lower wetland subenvironment (Figs. 3, 6f), the palynoflora is characterized by a dominance of gymnospermous pollen grains including *Alisporites* sp., *Araucariacites australis* Cookson, *Callialasporites dampieri* (Balme) Dev, *C. trilobatus* (Balme) Dev, *C. turbatus* (Balme) Schulz, *Classopollis classoides* (Pflug) Pocock and Jansonius, *C. simplex* (Danzé, Corsin and Laveine) Reiser and Williams, *Ephedripites* sp., *Microcachryidites castellanosii* Menéndez, and *Podocarpidites* sp. (Fig. 7e–l). Among these taxa, Cheirolepidiaceae (*Classopollis* spp.) pollen constitutes approximately 82% of the total assemblage, with many tetrad forms (Fig. 7f) indicating that this pollen represents the local flora. Trilete fern spores (*Leptolepidites macroverrucosus* Schulz, *L. verrucatus* Couper, and *Uvaesporites* sp.) also occur in monads and tetrads (Fig. 7a–d). These cheirolepidiacean and fern species would have grown around small freshwater bodies where green coccal algae (*Botryococcus* sp.) developed (Fig. 9). The producers of the Araucariacean pollen types (*Callialasporites* spp. and *Araucariacites* sp.) and the pteridosperms (*Alisporites* sp.) would have inhabited more elevated areas close to the bodies of water (Fig. 9). The presence of *Classopollis* spp. and *Ephedripites* sp. indicates an arid macroenvironment, whilst the former is also an indicator of warm to warm temperate climates and well-drained soils.

In the upper wetland subenvironment (Figs. 3, 6g–h), the association shows a strong dominance of aquatic species (86% of the total assemblage). The most conspicuous forms are the green algae *Botryococcus* sp. (Fig. 7m–o), which appear together with *Ovoidites* sp. This overwhelming dominance of the planktonic *Botryococcus* sp. indicates a freshwater environment where the benthonic *Ovoidites* sp. would also have developed. Hygrophile (*sensu* Remy and Remy, 1977) elements complete the local palynoflora, with trilete spores from ferns (*Deltoidospora* sp.) that would have grown on the borders of the water bodies.

5.2. Palaeoinvertebrates

The palaeoinvertebrate faunal association from the Puesto Almada Member is one of the most diverse from Jurassic rocks in Argentina and from the southern hemisphere as a whole. In fact, there are only three other insect faunas recorded from the Gondwana realm (from Australia, India, and Antarctica) (Gallego and Martins Neto, 1999).

5.2.1. Spinicaudatans ('conchostracans')

The first studies of the 'conchostracan' fauna from the Cañadón Asfalto Formation were carried out by Piatnitzky (1936), who reported on high quantities of 'conchostracans' and named this succession "Estratos con *Estheria*" (Beds with *Estheria*). The first descriptions of spinicaudatans from the Las Chacritas Member were published by Tasch and Volkheimer (1970). Fourteen species of Jurassic spinicaudatans have now been described, with ten of these from the Cañadón Asfalto Formation (Tasch and Volkheimer, 1970; Vallati, 1986; Gallego, 1994; Gallego et al., 2010, 2011). Among them, *Congestheriella rauhuti* has been previously described in several localities of the Puesto Almada Member, including Cerro Bandera (Gallego et al., 2010).

The spinicaudatan records consist of *Congestheriella rauhuti* (the most abundant species; Fig. 8a), as well as new specimens that have been assigned to Euestheriidae (Fig. 8b), Anthronestheriidae (*Pseudestherites* sp.), and Palaeolimnadiopseidae (Fig. 8c). *Congestheriella rauhuti* is preserved as isolated and complete carapace impressions. It is remarkable that each spinicaudatan association at the Cerro Bandera locality (Euestheriidae, Anthronestheriidae, and Palaeolimnadiopseidae) is monospecific. The 'conchostracan' fauna vary greatly between the different wetland subenvironments in terms of their dimensions and abundances, which probably were caused by genetic variability or else primarily by ecological conditions in their microenvironments. The smallest species (*Congestheriella rauhuti*) was recorded in sediments corresponding to shallow water bodies (Lacustrine facies association; Fig. 2) whilst the largest (Euestheriidae, Anthronestheriidae, and Palaeolimnadiopseidae) were found in the wetlands suggesting a larger food and water supply (Claystones and silstones facies; Fig. 3).

5.2.2. Insects

The Jurassic insect faunas of Argentina are less known than the Triassic ones, due to their restricted stratigraphic distribution, low number of known fossiliferous localities, and species diversity. Records for Jurassic assemblages have been published by a variety of authors (Gallego et al., 2011 and references therein), with the presence of the orders Coleoptera (elytra and body parts), ?Hemiptera (wing fragment), and Trichoptera (wings and larval cases) being reported from the La Matilde and Cañadón Asfalto Formations. For the latter, Andrade-Morraye and Genise (2005) and Petrulevicius (2007) mentioned the presence of chironomid head capsules and larval cases, and mecopterans (Bittacidae), respectively; however not including the exact stratigraphic provenances in the Gan Gan area (Fig. 1).

The insect body records from the studied section belong to the Hemiptera (Fig. 8d) and Coleoptera orders as well as the remains of caddisfly fossil cases from the order Trichoptera. The caddisfly specimens mainly consist of cases belonging to the ichnogenera *Folindusia* (Berry), *Conchindusia* (Vialov and Sukatcheva), and *Terrindusia* (Vialov) (Fig. 8e). These fossils are preserved as imprints or compressed moulds. The trichopterans indicate well-oxygenated stream environments, therefore they are considered allochthonous to the wetland environments where they are found (Fig. 3). Hemipterans present morphological characteristics (large coxal insertion and abdomen width; Fig. 8d) that resemble aquatic forms.

5.2.3. Ostracods

Ostracod faunas from the Cañadón Asfalto Formation had been studied and reviewed by various authors during the last two decades, and three monospecific genera have been identified: *Penthesilenula sarytirmenensis* (Sharapova), *Theryosinoecum barrancalensis minor* Musacchio, Beros and Pujana, and *Mandelstamia*? (see in Ballent and Díaz, 2011; Gallego et al., 2011). In the section studied here, the Darwinuloidea *Penthesilenula sarytirmenensis* and the Cytheroidea *Theryosinoecum barrancalensis minor* are found in the Lacustrine and Palustrine facies associations (Fig. 9). These specimens are small and abundantly preserved as mould remains.

Interpretation: The complete faunal association from the Puesto Almada Member in the Cerro Bandera locality reflects the presence of shallow, low energy freshwater environments (palustrine; Fig. 9), with associated plant communities.

6. Discussion

6.1. Depositional system

The facies and their associations represent processes that formed part of the deposition in a carbonate-rich lacustrine system that was surrounded by palustrine areas associated with an alluvial fan and fluvial system, and an alluvial plain environment (Fig. 9). The succession (alluvial–fluvial–lacustrine) is characteristic of deposition in rift basins (Gawthorpe and Leeder, 2000). Moreover, the littoral subenvironment of the carbonate lake was influenced by deposition of pyroclastic material, creating mixed pyroclastic–carbonate sediments. This also reflects a common feature of rift basins with important volcanism (Cabaleri et al., 2010a) (Fig. 9).

The nature of the lake was ephemeral as evidenced by the abundant and widespread subaerial exposure features (cracking, superimposed pedogenesis, and gypsum layers) in the succession that represent periods of low lake level during the contraction of the water bodies. As reflected by bed geometry, the system was limited in extent, more likely reflecting pond settings. A similar model was proposed for the Cañadón

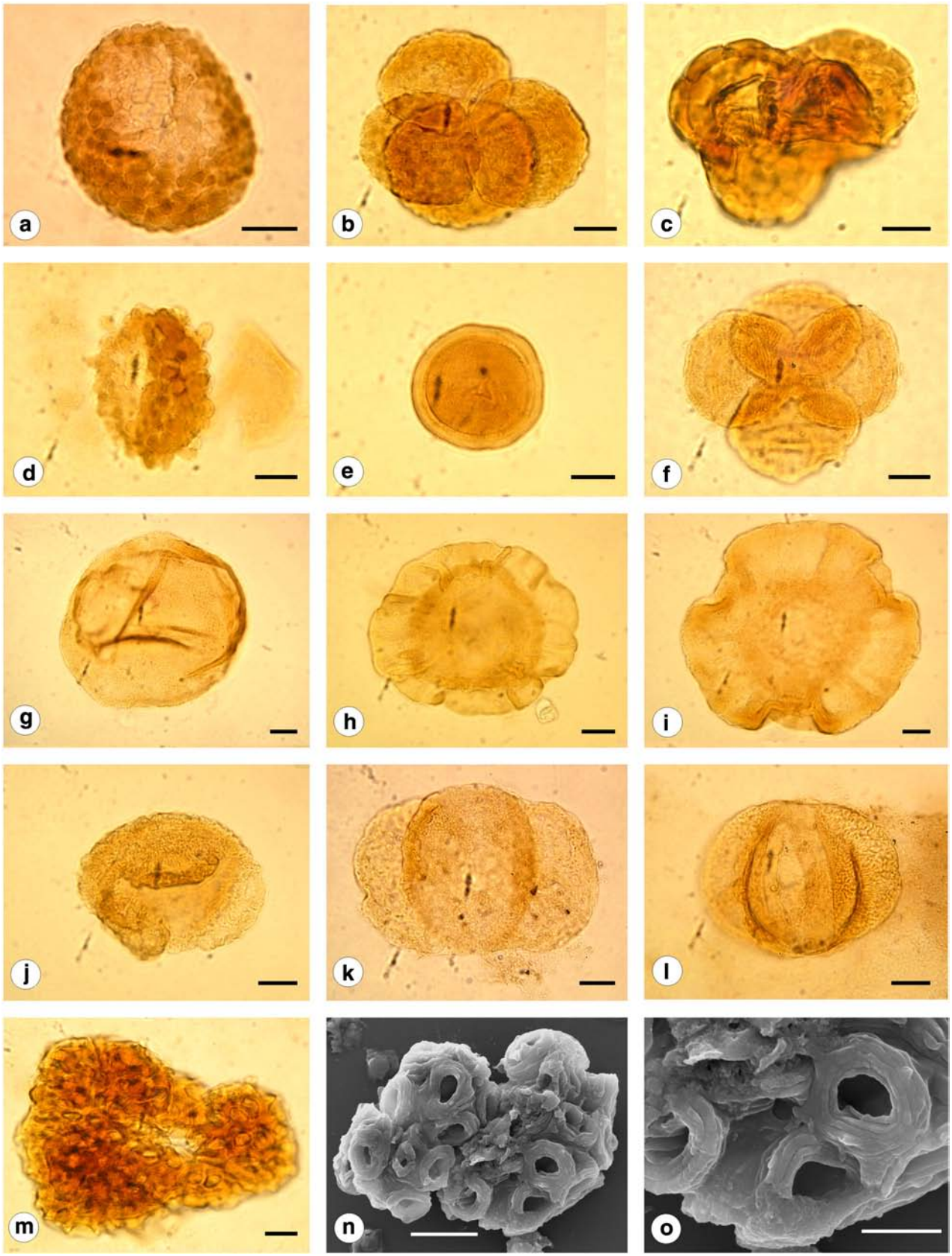

Fig. 7. Palynomorph assemblage from the Puesto Almada Member in Cerro Bandera locality. a *Leptolepidites verrucatus*, monad, 7678 F: W30/1 MPLP; b *Leptolepidites verrucatus* Couper, tetrad, 7677E: O41/2 MPLP; c *Leptolepidites macroverrucosus* Schulz, tetrad 7680B: S30/1 MPLP; d *Uvaesporites* sp., 7678I: V42/2 MPLP; e *Classopollis simplex* (Danzé, Corsin and Laveine) Reiser and Williams, 7678D: O39/1 MPLP; f *Classopollis classoides* (Pflug) Pocock and Jansonius, tetrad, 7677E: R45/1 MPLP; g *Araucariacites australis* Cookson, 7677E: E30 MPLP; h *Callialasporites dampieri* (Balme) Dev, 7678D: T27/2 MPLP; i *Callialasporites trilobatus* (Balme) Dev, 7678D: Y394 MPLP; j *Microcachryidites castellanosii* Menéndez, 7677 F: T39/1 MPLP; k *Podocarpidites* sp., 7677D: W26/3 MPLP; l *Alisporites* sp., 7678C: L37/2 MPLP; m *Botryococcus* sp., 9624G: T39/3 MPLP; n *Botryococcus* sp., MEB MACN; o *Botryococcus* sp., detail of *n*, MEB MACN. Scale bars = 10 μm.

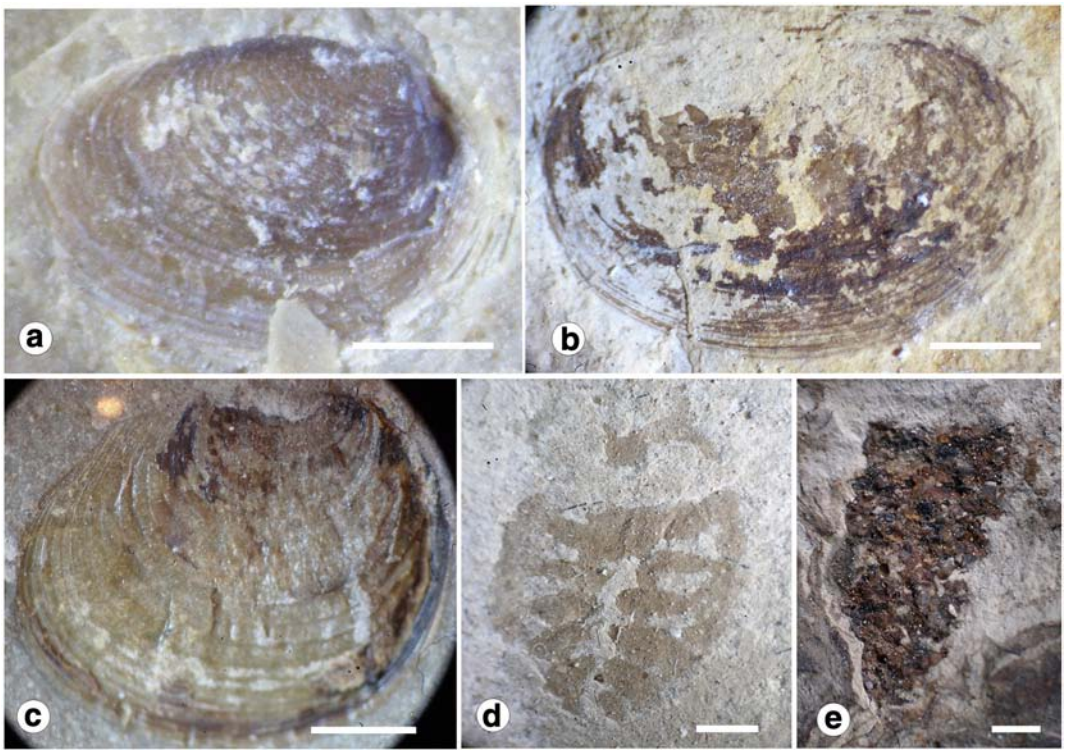

Fig. 8. Invertebrate fauna from the Cerro Bandera locality, Puesto Almada Member, Cañadón Asfalto Formation. Spinicaudata, a *Congestheriella rauhuti*; b Euestheriidae; c Palaeolimnadiopseidae; Insecta, d Hemiptera body; e Caddisfly cases. Scale bars = 1 mm.

Asfalto Formation at the Cerro Cóndor sub-basin where a hydrologically closed ephemeral palaeolake was defined by Cabaleri et al. (2005). Also recently, a dominantly palustrine–lacustrine carbonate environment has been described for the Las Chacritas Member in the Fossati sub-basin (Cabaleri and Benavente, 2013).

Early studies of saline–alkaline lakes revealed a common pattern of mineralogical zoning, which was interpreted as a consequence of laterally variable water chemistry (Hay, 1966; Sheppard and Gude, 1969). This zoning, which forms a sort of "bull's eye" depositional pattern, consists of alkali silicic zeolites such as clinoptilolite, erionite, and phillipsite precipitating in the margins, grading into analcime, then followed by potassium feldspar in the centres of the lakes. There is a general consensus that analcime forms by replacement of earlier zeolites, including clinoptilolite (Wilkin and Barnes, 1998). Moreover, volcanic glass is the most frequent precursor of zeolites in saline–alkaline lakes (Surdam and Sheppard, 1978; Boles and Surdam, 1979). In the case of the inferred Fossati wetlands, we cannot be sure whether analcime formed directly from volcanic glass or by replacement of a primary zeolite, since clinoptilolite/heulandite was identified (with uncertainty) in only one of the levels studied. However, the widespread occurrence of analcime in the wetland sediments corresponding to the palustrine areas, suggests persistently alkaline–brackish water. This is in contrast with the high salinity conditions defined for the Cerro Cóndor palaeolake (Cabaleri et al., 2005).

The *Microcodium* in these ponds is thought to be allocthonous and indicates proximity to marginal areas with palaeosol development (Arribas et al., 1996). The inferred palustrine environments related to the marginal zone of the postulated palaeolakes are characterized by primary subaqueous features strongly modified by posterior subaerial exposure (Alonso-Zarza and Wright, 2010). The exposure was most likely triggered by rising and falling of the water table (Meléndez et al., 2009), which also caused the formation of pisolites and structures originated in the vadose freshwater environment (Alonso-Zarza, 2003). Similar facies associations have been proposed for carbonate lakes with associated palustrine settings from the Mesozoic and Cenozoic of Spain (Alonso-Zarza and Calvo, 2000; Meléndez et al., 2009; Alonso-Zarza et al., 2012), as well as from wetlands (Dunagan and Turner, 2004), and alluvial fans (Turner and Peterson, 2004). In the Puesto Almada palustrine setting, the presence of calcified root moulds, fenestral and alveolar structures, and *Microcodium*, indicate the influence of a vegetation cover, either as aquatic plants in the ponds or as terrestrial plants in the marginal zones, and the incipient formation of soils (Vázquez-Urbez et al., 2002; Arenas et al., 2007; Alonso-Zarza and Wright, 2010) (Fig. 9). This pedogenic development occurred during times of exposure (low water levels), when the wetland/lake complex suffered minor evaporitic processes (Dunagan and Turner, 2004). The presence of cyanobacteria-like algae in the ponds, allowed the formation of giant oncoids (Fig. 5d–e) by covering the stems and roots of submerged macrophytes. This biogenically-mediated process has been described before in similar depositional settings (Arenas et al., 2007; Arenas-Abad et al., 2010; Benavente et al., 2012).

The presence of filter-feeding and suspension-feeding invertebrates as found by us in these inferred settings, such as ostracods, and 'conchostracans', confirms optimal conditions for the development of invertebrate populations and also suggests well oxygenated conditions (Dunagan and Turner, 2004). Nevertheless, the ponds and wetlands suffered recurrent anoxic conditions, as reflected by the presence of preserved OM and carbonaceous impressions of plants.

The Puesto Almada Member reflects deposition during the *sag* stage of the rift basin formation when tectonic activity had reached relative stability and subsidence was generated mainly by thermal factors (Gawthorpe and Leeder, 2000). The geometry of the facies, and variations in their lateral distributions, indicate sedimentation in a small sub-basin where there was a balanced ratio between the sediment supply and the accommodation space. A different situation is recognized upwards in the succession with the progradation of the fluvial systems into the lake environment (Fig. 2). This accounts for a sediment supply greater than the accomodation space and therefore low subsidence (Cabaleri et al., 2010a). Our interpretation is that these less balanced ratios were the result of the resumption of tectonic activity in the Lower

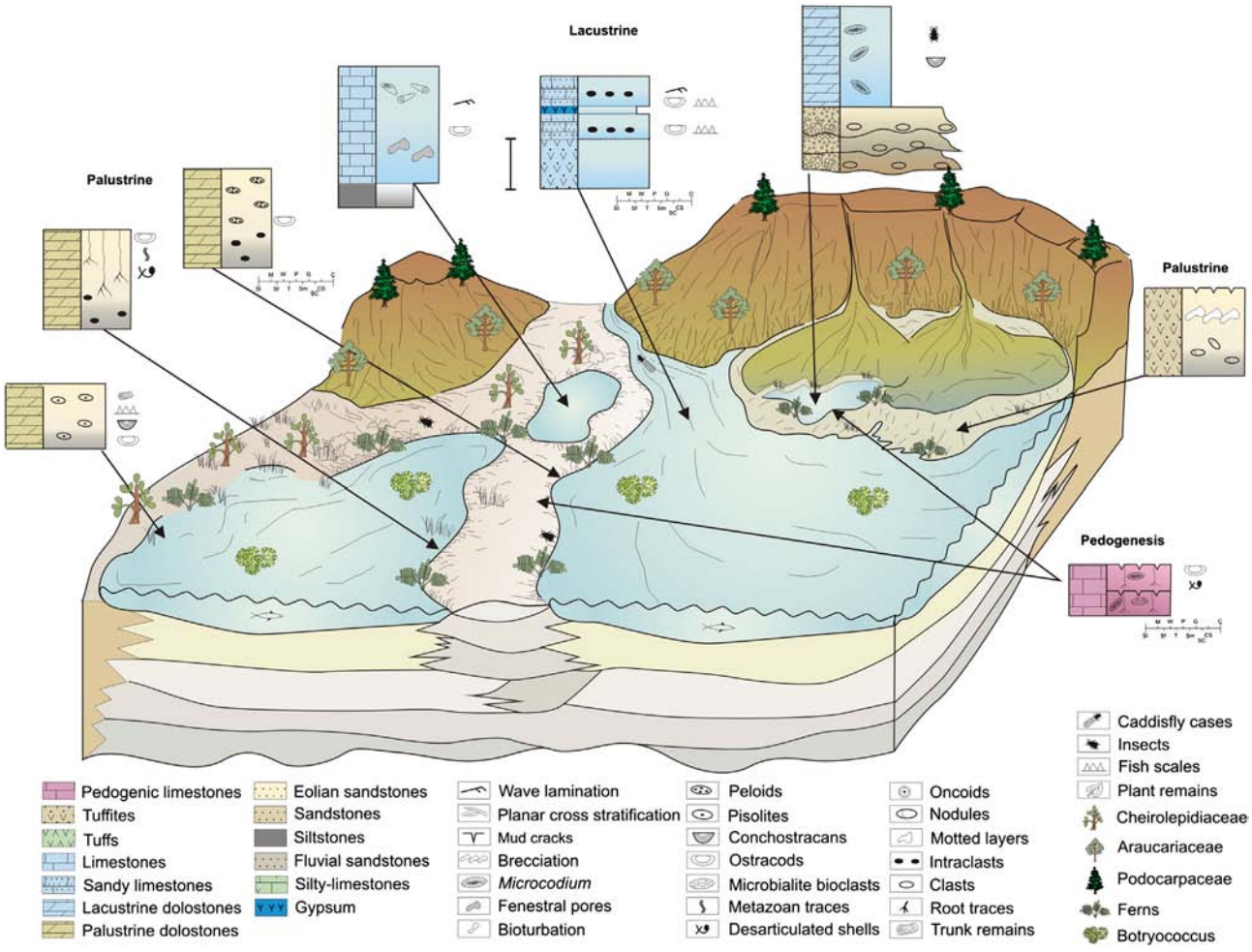

Fig. 9. Schematic palaeoenvironmental facies model proposed for the lacustrine system of the Puesto Almada Member, Cañadón Asfalto Formation (Jurassic) at Cerro Bandera locality; showing the palynological and palaeoinvertebrate contents.

Cretaceous (Ranalli et al., 2011). Cabaleri and Benavente (2013) found the opposite for the Las Chacritas Member that was apparently deposited during the *synrift* stage of the basin, which indicates a predominant tectonic control on sedimentation. Nevertheless, in the upper section of the Las Chacritas Member, a decrease in the creation of accommodation had already been detected. This trend towards low subsidence and minor tectonic control over sedimentation continues during the Puesto Almada Member deposition. Under such a tectonic context, it is plausible to propose that the sedimentology observed in the succession of the Puesto Almada Member directly reflects the climate conditions prevalent for the time of deposition in the Fossati sub-basin.

Shallowing upward successions were observed for the Las Chacritas Member in the Fossati sub-basin (Cabaleri and Benavente, 2013). The successions are capped by palaeosols that represent subaerial exposure events; these deposits constitute the bounding surfaces of the successions. The successions were mainly controlled by changes in climatic variables. In the third succession, the deposits of an alluvial fan system are represented by the Alluvial fan matrix-supported conglomerates and fluvial sandstones facies association. This system is the only record of alluvial evidence in the entire Cañadón Asfalto Basin. According to Bohacs et al. (2000), this succession represents a climate-tectonic balanced control of sedimentation.

6.2. Jurassic palaeoclimates and palaeoenvironments in Patagonia

The Mesozoic was characterized by particularly warm climate associated with high levels of CO_2 (~2000 ppm), and with cold pulses that each lasted less than 3 Ma (Royer, 2006). During the Jurassic, South America was part of the Gondwana supercontinent. Compagnucci (2011) explains that since the Jurassic and up until the present, the Patagonian climate "is conditioned by the southern borders of the semipermanent anticyclons of the Southern Atlantic and Pacific oceans, which extend southward to approximately 30°S to 38°S, or even further south, as a result of the flux of the westerlies". These prevailing westerlies continue to be one of the most distinctive climatic features of Patagonia today.

Rees et al. (2000) studied the morphology and distributional patterns of fossil leaves and lithologies such as coals and evaporites and recognized five main biomes for the Jurassic: 1) seasonally dry (summer wet), 2) desert, 3) seasonally dry (winter wet), 4) warm temperate biomes, and 5) cool temperate biomes (see Fig. 7 in Rees et al., 2000). These authors analysed two extreme vegetation types: localities comprising wholly microphyllous forms (of conifers and cycadophytes), and localities comprising wholly macrophyllous conifers and ginkgophytes. Microphyllous plant localities occur at low palaeolatitudes and can be assigned to a seasonally hot and dry condition (biome 1), consistent with evaporites and aeolian sand transport. The macrophyllous conifer/ginkgophyte localities occur at high palaeolatitudes and can be assigned to seasonally cool and/or darker conditions (biome 5), based upon the deciduous nature of the foliage. It is harder to define the latitudinal boundaries between these two biomes and the intermediate warm temperate biome. However, the occurrence of macrophyllous cycadophytes and ferns, the changes seen in their relative abundance with respect to microphyllous and ginkgophyte forms, and coal distributions, enable subdivisions of the floral and climate spectrum (Rees et al., 2000).

The floras in Argentina and the Antarctic Peninsula belong to the same seasonally dry-winter wet biome for the Middle Jurassic (Rees et al., 2000). In a study on palynobiotas of the Middle Jurassic in Patagonia, Quattrocchio et al. (2011) mention three main groups of gymnosperms: the cheirolepidiaceans, which inhabit warm and semi-arid lowlands with well-drained soils; the araucariaceans, growing in more or less humid biotopes at different altitudes, and the podocarpacean forest, which covers more elevated areas. In the Las Chacritas Member at the Cañadón Lahuincó locality (Cerro Cóndor sub-basin), Volkheimer et al. (2008) recorded an algal assemblage composed of planktonic (*Botryococcus*) and non-planktonic green algae (represented by the *Spirogyra*-like spores of the genus *Ovoidites*). Both of these taxa indicate shallow lake levels, and probably saline conditions. They appear along with high percentages of *Classopollis* spp. (thermophilic Cheirolepidiaceae) indicating warm climate and well-drained soils around the lakes. Cabaleri et al. (2010a) have defined a wet palaeoenvironment for the Las Chacritas Member, with development of a palaeolake with an extensive littoral (deep, shallow, and eulittoral) and marginal (supralittoral and palustrine) areas.

In general, the palustrine limestones hold rich information about palaeoenvironmental conditions (Platt and Wright, 1992). In the Puesto Almada Member studied here, these layers are abundant and are recognized by the presence of widespread mud cracks, nodules, and pedogenesis. They all undoubtedly indicate subaerial exposure and desiccation and resemble analogous characteristics described for the Las Chacritas Member, and they also fit into the intermediate area between arid and sub-humid climate type conditions defined by Platt and Wright (1992). Moreover, mineralogical data show that smectite predominated in the palaeoenvironments, indicating aridity (Kraus and Hasiotis, 2006).

Furthermore, for the Las Chacritas Member, the presence of extensive stromatolites, developed in several localities is relevant. The planar stromatolite facies and the fenestral fabric, reflect metabolic activity of benthic microbial communities, dominated by cyanobacteria that grew in a eulittoral environment with poor water agitation (Cabaleri et al., 2005). Also, the presence of this stromatolite facies implies low energy conditions with high salinity and alkalinity, and warm temperatures and humid conditions (Freytet, 2000). However, there are also numerous levels with mud cracks and evaporite minerals (Table 3), which reflect drying.

In the Puesto Almada Member, there are no stromatolitic strata. Probably, the fluvial and alluvial facies represent major superficial water supply through seasonal precipitation, with higher levels of water agitation and sediment supply preventing the development of stromatolites. Limestones are less frequent and are overlain by tuffs, sandy-tuffites, and laminated sandstones, with red being the dominant colour in several localities (Cabaleri et al., 2010a). The only microbialitic facies recognized contaINS mega-oncoids. These include sponge gemmules, which indicate an unstable environment, as they could be an adequate solution for survival (Ott and Volkheimer, 1972). The oncolitic limestones present pedogenic features such as interbedded evaporative layers, mud cracks and rizoliths, indicating desiccation (Cabaleri et al., 2010a) (Table 3). These conditions reflect the palaeolake contraction, indicating a more arid palaeoclimate than during the Las Chacritas deposition.

7. Conclusions

In the Upper Jurassic Puesto Almada Member (Canadón Asfalto Formation) at the Cerro Bandera locality, the various facies/microfacies correspond to a carbonate alkaline palustrine–lacustrine system with associated alluvial fan and fluvial systems. The facies associations constitute four shallowing upward successions defined by local exposure surfaces characterized by: 1) a Lacustrine–Palustrine-Pedogenic facies association with a 'conchostracan' (*Congestheriella rauhuti*)–ostracods (*Penthesilenula sarytirmenensis*, *Theryosinoecum barrancalensis minor*) association; 2) a Palustrine facies association representing a wetland subenvironment, and yielding 'conchostracans' (Euestheriidae), body remains of insects (Hemiptera and Coleoptera), fish scales, ichnofossils (*Folindusia* and *Terrindusia*), and palynomorphs (cheirolepidiacean species and ferns probably growing around water bodies, and other gymnosperms in more elevated areas); 3) an Alluvial fan facies association indicating the area of sediment supply; and 4) a Lacustrine facies association representing a second wetland episode, and yielding 'conchostracans' (Palaeolimnadiopseidae), insect ichnofossils (*Conchindusia*), and a palynoflora mainly consisting of planktonic green algae associated with hygrophile elements.

Climate was a predominant control on deposition of the Puesto Almada Member with tectonics playing a minor role in the evolution

Table 3
Chart summarizing the sedimentological evidence supporting the climatic condition interpretations (dry or wet) from various localities of the Las Chacritas and Puesto Almada Members (Cañadón Asfalto Formation).

	Las Chacritas Member			Puesto Almada Member		
Sub-basin	Locality	Dry evidence	Wet evidence	Locality	Dry evidence	Wet evidence
Cerro Cóndor (Cabaleri et al., 2010a; Gallego et al., 2011)	Cañadón Las Chacritas (Type locality)	Mud cracks (three levels) Gypsum and calcite laminae	Subaqueous diagenesis in stromatolite facies Coal	Estancia El Torito (Type locality)	Mud cracks (four levels) Gypsum and calcite laminae	Bituminous shales
	Cañadón Asfalto	Mud cracks (five levels) Gypsum and calcite laminae	Bituminous shales Subaqueous diagenesis in stromatolite facies	Cañadón Asfalto	Mud cracks (five levels)	–
	Cañadón Lahuincó	Gypsum and calcite laminae Mud cracks (one level)	Bituminous shales Subaqueous diagenesis in stromatolite facies	Cañadón Lahuincó	–	–
	Cañadón Los Loros	Mud cracks (six levels)	Subaqueous diagenesis in stromatolite facies	Cañadón Los Chivos	–	Bituminous shales
	Sierra de Pichiñanes	Mud cracks (five levels)	Stromatolite facies Sinter	Cañadón Limonao	Mud cracks (three levels)	Bituminous shales
	Cañadón Miyanao	Mud cracks (five levels) Gypsum and calcite laminae	Bituminous shales Stromatolite facies	Estancia La Sin Rumbo	Mud cracks (twelve levels)	Bituminous shales
	Cañadón Carrizal	Mud cracks (one level) Gypsum in stromatolite facies	Subaqueous diagenesis in stromatolite facies	–	–	–
	Sierra de La Manea	Mud cracks (seven levels)	Shales			
Fossati	Estancia Fossati (in prep)	Mud cracks (one level)	Subaqueous diagenesis in stromatolite facies	Cerro Bandera (this paper)	Mud cracks (one level)	Bituminous shales

of the depositional system. The presence of wetlands and lacustrine facies could indicate humid conditions with a rate of precipitation that was sufficiently greater than evaporation for the development of biota and stable aquatic systems. The fluvial and alluvial facies represent the operation of seasonal precipitation that reflects differences in seasonality patterns between the Las Chacritas and Puesto Almada Members, with seasonality being stronger in the latter.

The invertebrate palaeontological studies reveal the first record of fossil insect bodies (Insecta-Hemiptera and Coleoptera), being found in association with caddisfly cases (Insecta-Trichoptera), ostracods (Crustacea), and spinicaudatans (Crustacea–Branchiopoda–'conchostracans') for the Cañadón Asfalto Formation. This record is one of the most diverse from Jurassic rocks in Argentina and from the southern hemisphere.

The sedimentological, mineralogical, and palaeontological data discussed are consistent with proposed climatic models for the Upper Jurassic (Compagnucci, 2011; Iglesias et al., 2011), which indicate an arid climate for extra-Andean Patagonia. In particular, strong seasonality is inferred for the Puesto Almada Member in the Fossati sub-basin and the presence of wetlands and lacustrine sediments could indicate periods of more humid conditions. Nevertheless, further studies from new localities within this sub-basin and others are necessary, in order to continue to build a regional palaeoclimatic framework for the Cañadón Asfalto Basin.

Acknowledgements

This study was supported by the grants of Consejo Nacional de Investigaciones Científicas y Técnicas (CONICET) No 5760, 112-201001-00034 (NC) and 5581 (OFG). The authors wish to thank A. Alonso-Zarza for reviewing an earlier version of the manuscript. The comments of the reviewers H. Corlett and P. Eriksson are kindly acknowledged. B. Jones and M. Isaac are thanked for their editorial assistance. The Comisión Nacional de Energía Atómica (CNEA) provided the logistic support at the Campamento Los Adobes and C. Armella collaborated during fieldtrips. Mr. and Mrs. Fossati are thanked for providing access to Estancia Fossati. E. Llambias prepared the rock thin sections and G. Giordanengo the digital figures. J. Coil (Berkeley Cross-Cultural Associates) revised the English of the manuscript.

References

Alonso-Zarza, A.M., Calvo, J.P., García del Cura, M.A., 1992. Palustrine sedimentation and associated features grainification and pseudo-microkarst in the Middle Miocene (Intermediate Unit) of the Madrid Basin, Spain. Sediment. Geol. 76, 43–61.

Alonso-Zarza, A.M., 2003. Palaeoenvironmental significance of palustrine carbonates and calcretes in the geological record. Earth Sci. Rev. 60 (3–4), 261–298.

Alonso-Zarza, A.M., Arenas, C., 2004. Cenozoic calcretes from the Teruel Graben, Spain: microstructure, stable isotope geochemistry and environmental significance. Sediment. Geol. 167, 91–108.

Alonso-Zarza, M.A., Calvo, J.P., 2000. Palustrine sedimentation in an episodically subsiding basin: the Miocene of the northern Teruel Graben (Spain). Palaeogeogr. Palaeoclimatol. Palaeoecol. 160, 1–21.

Alonso-Zarza, A.M., Wright, V.P., 2010. 2 Palustrine Carbonates. In: Alonso-Zarza, A.M., Tanner, L. (Eds.), Carbonates in continental settings. Facies, environments and processes. Developments in Sedimentology, 61. Elsevier, Amsterdan, pp. 103–131.

Alonso-Zarza, A.M., Meléndez, A., Martín-García, R., Herrero, M.J., Martín-Pérez, A., 2012. Discriminating between tectonism and climate signatures in palustrine deposits: lessons from the Miocene of the Teruel Graben, NE Spain. Earth Sci. Rev. 113, 141–160.

Andrade-Morraye, M., Genise, J., 2005. An association of fossil larval tubes and head capsules of Chironomidae (Diptera) from the Jurassic (Callovian–Oxfordian) Cañadón Asfalto Formation, Patagonia, Argentina. Proceedings of the Fossils X3. International Paleoentomological Society, Pretoria, p. 5.

Arenas, C., Cabrera, L., Ramos, E., 2007. Sedimentology of tufa facies and continental microbialites from the Palaeogene of Mallorca Island (Spain). Sediment. Geol. 197, 1–27.

Arenas-Abad, C., Vázquez-Urbez, M., Pardo-Tirapu, G., Sancho-Marcén, C., 2010. Fluvial and associated carbonate deposits. In: Alonso-Zarza, A.M., Tanner, L. (Eds.), Carbonates in continental settings. Facies, environments and processes. Developments in Sedimentology, 61. Elsevier, Amsterdan, p. 176.

Armenteros, I., Daley, B., Garcia, E., 1997. Lacustrine and palustrine facies in the Bembridge Limestone (late Eocene, Hampshire Basin) of the Isle of Wight, southern England. Palaeogeogr. Palaeoclimatol. Palaeoecol. 128, 111–132.

Arp, G., 1995. Lacustrine bioherms, spring mounds and marginal carbonates of the ries-impact-crater (Miocene, Southern Germany). Facies 33, 35–90.

Arribas, M.E., Estrada, E., Obrador, A., Rampone, G., 1996. Distribución y ordenación de *Microcodium* en la Formación Tremp: Anticlinal de Campllong (Pirineos Orientales, provincial de Barcelona). Rev. Soc. Geol. Esp. 9, 9–18.

Ballent, S.C., Díaz, A.R., 2011. Contribution to the taxonomy, distribution and paleoecology of the early representatives of *Penthesilenula* Rossetti & Martens, 1998 (Crustacea, Ostracoda, Darwinulidae) from Argentina, with the description of a new species. Hydrobiologia. http://dx.doi.org/10.1007/s10750-011-0658-8.

Benavente, C.A., Mancuso, A.C., Cabaleri, N.G., 2012. First occurrence of charophyte algae from a Triassic Paleolake in Argentina and their paleoenvironmental context. Palaeogeogr. Palaeoclimatol. Palaeoecol. 363–364, 172–183.

Bohacs, K.M., Carrol, A.R., Neal, J.E., Mankiewickz, P.J., 2000. Lake-Basin Type, Source Potential, and Hydrocarbon Character: an Integrated Sequence-Stratigraphic–Geochemical Framework. In: Gierlowski-Kordesch, E.H., Kelts, K.R. (Eds.), Lake basins through space and time. AAPG Studies in Geology, 46, pp. 3–34.

Boles, J.R., Surdam, R.C., 1979. Diagenesis of volcanogenic sediments in a Tertiary saline lake; Wagon Bed Formation, Wyoming. Am. J. Sci. 279, 832–853.

Bromley, R.G., 1996. Trace Fossils. Biology, Taphonomy and Applications.Chapman and Hall, London (361 pp.).

Buatois, L., Mángano, M.G., 1998. Trace fossil analysis of lacustrine facies and basins. Palaeogeogr. Palaeoclimatol. Palaeoecol. 140, 367–382.

Busquets, P., Méndez-Bedia, I., Gallastegui, G., Colombo, F., Heredia, N., Cardó, R., Limarino, O., 2007. Late Palaeozoic microbial lacustrine carbonate and related volcanic facies from the Andean Frontal Cordillera (San Juan, Argentina). Cuadernos del Museo Geominero, 8 69–74.

Bustillo, M.A., Alonso-Zarza, A.M., 2007. Overlapping of pedogenesis and meteoric diagenesis in distal alluvial and shallow lacustrine deposits in the Madrid Miocene Basin, Spain. Sediment. Geol. 198, 255–271.

Cabaleri, N., Armella, C., 1999. Facies lacustres de la Formación Cañadón Asfalto (Caloviano-Oxfordiano) en la quebrada Las Chacritas, Cerro Cóndor, provincia del Chubut. Rev. Asoc. Geol. Argent. 5, 377–388.

Cabaleri, N.G., Benavente, C.A., 2013. Sedimentology and paleoenvironments of the Las Chacritas carbonate palaeolake, Cañadón Asfalto Formation (Jurassic), Patagonia Argentina. Sed. Geol. 284–285, 91–105.

Cabaleri, N., Armella, C., Silva Nieto, D.G., 2005. Saline lakes of Cañadón Asfalto (Middle Upper Jurassic), Cerro Cóndor, Chubut Province (Patagonia), Argentina. Facies 51, 350–364.

Cabaleri, N., Armella, C., Silva Nieto, D., Volkheimer, W., 2006. Paleoambientes sedimentarios de la Formación Cañadón Asfalto (Jurásico Superior) en los depocentros de Cerro Cóndor y Gastre - Gan Gan Provincia del Chubut. Resúmenes 4º Congreso Latinoamericano de Sedimentología y 11º Reunión Argentina de Sedimentología. Asociación Argentina de Sedimentología, Buenos Aires, p. 64.

Cabaleri, N., Volkheimer, W., Armella, C., Gallego, O., Silva Nieto, D., Paez, M., Cagnoni, M., 2008. Continental aquatic environments of the Jurassic in extraandean Patagonia. Resúmenes 12º Reunión Argentina de Sedimentología. Asociación Argentina de Sedimentología, Buenos Aires, p. 47.

Cabaleri, N.G., Volkheimer, W., Armella, C., Gallego, O.F., Silva Nieto, D.G., Cagnoni, M.C., Ramos, A.M., Panarello, H.O., Paez, M., Koukharski, M., 2010a. Estratigrafía, análisis de facies y paleoambientes de la Formación Cañadón Asfalto en el Depocentro jurásico Cerro Cóndor, provincia del Chubut, Republica Argentina. Rev. Asoc. Geol. Argent. 66, 349–367.

Cabaleri, N., Volkheimer, W., Silva Nieto, D., Armella, C., Cagnoni, M., Hauser, N., Matteini, M., Pimentel, M.M., 2010b. U–Pb ages in zircons from Las Chacritas and Puesto Almada members of the Jurassic Cañadón Asfalto Formation, Chubut province, Argentina. Proceedings of the 7th South American Symposium on Isotope Geology. Universidade de Brasilia, Brasilia, pp. 190–193.

Cabaleri, N.G., Armella, C., Benavente, C.A., Monferran, M., Cagnoni, M., Gallego, O.F., Volkheimer, W., Silva Nieto, D.G., Páez, M.A., 2011. Evento carbonático multicíclico en el Jurásico Medio lacustre de la Patagonia central. Resúmenes 18º Congreso Geológico Argentino. Asociación Geológica Argentina, Neuquén, p. 2.

Codignotto, J., Nullo, F., Panza, J.L., Proserpio, C., 1979. Estratigrafía del Grupo Chubut entre Paso de Indios y Las Plumas, provincia del Chubut, Argentina. Actas 7º Congreso Geológico Argentino. Asociación Geológica Argentina, Neuquén, pp. 471–480.

Compagnucci, R.H., 2011. Atmospheric circulation over Patagonian from the Jurassic to present: a review through proxy data and climatic modeling scenarios. Biol. J. Linn. Soc. 103, 229–249.

Cuadros, J., Caballero, E., Huertas, J., Jiménez de Cisneros, C., Huertas, F., Linares, J., 1999. Experimental alteration of volcanic tuff: smectite formation and effect on ^{18}O isotope composition. Clays Clay Miner. 47, 769–776.

Cúneo, R., Ramezani, J., Scasso, R., Pol, D., Escapa, I., Zavattieri, A.M., Bowring, S.A., 2013. High-precision U–Pb geochronology and a new chronostratigraphy for the Cañadón Asfalto Basin, Chubut, central Patagonia: Implications for terrestrial faunal and floral evolution in Jurassic. Gondwana Res. http://dx.doi.org/10.1016/j.gr.2013.01.010.

Demko, T.M., Currie, B.S., Nicoll, K.A., 2004. Regional paleoclimatic and stratigraphic implications of palaeosols and fluvial/overbank architecture in the Morrison Formation (Upper Jurassic), Western Interior, USA. Sediment. Geol. 167, 115–135.

Dunagan, S.P., Turner, C.E., 2004. Regional paleohydrologic and paleoclimatic settings of wetland/lacustrine depositional systems in the Morrison Formation (Upper Jurassic), Western Interior, U.S.A. Sediment. Geol. 167, 271–298.

Faure, G., 1998. Principles and Applications of Geochemistry, 2nd edn. Prentice Hall, London (600 pp.).

Figari, E.G., Courtade, S.F., Constantini, L.A., 1996. Stratigraphy and tectonis of Cañadón Asfalto Basin, lows of Gastre and Gan Gan, north of Chubut province, Argentina. In: Riccardi, A.C. (Ed.), Advances in Jurassic Research. Transtec Publications, Hampshire, pp. 359–368.

Flügel, E., 2004. Microfacies and carbonate rocks. Analysis, interpretation and application. Springer, Berlin (975 pp.).

Folk, R.L., Andrews, P.B., Lewis, D.W., 1970. Detrital sedimentary rock classification and nomenclature for use in New Zealand. N. Z. J. Geol. Geophys. 13, 937–968.

Freyt, R., Pemberton, S.G., Fargestron, J.A., 1984. Morphological, ethological, and environmental significance of the ichnogenera Scoyenia and Ancorichnus. J. Paleontol. 58, 511–528.
Freytet, P., 2000. Distribution and paleoecology of non marine algae and stromatolites: II, the Limagne of Allier, Oligo–Miocene lake (Central France). Ann. Paleontol. 86, 3–57.
Freytet, P., Plaziat, J.C., 1982. Continental carbonate sedimentation and pedogenesis–Late Cretaceous and Early Tertiary of Southern France. In: Purser, B.H. (Ed.), Contributions to Sedimentology, 12. Verlag, Stuttgart, pp. 1–213.
Gallego, O.F., 1994. Conchóstracos Jurásicos de Santa Cruz y Chubut, Argentina. Ameghiniana 31, 333–345.
Gallego, O.F., Cabaleri, N.G., 2005. Conchóstracos de la Formación Cañadón Asfalto (Jurásico Medio – Superior): análisis preliminar de su distribución estratigráfica. II Simposio Argentino del Jurásico (Buenos Aires). Ameghiniana, 42, p. 51R.
Gallego, O.F., Martins Neto, R.G., 1999. La entomofauna mesozoica de Argentina. Estado actual del conocimiento. Rev. Soc. Entomol. Argent. 58, 86–94.
Gallego, O.F., Shen, Y.B., Cabaleri, N.G., Hernandez, M., 2010. The genus *Congestheriella* Kobayashi, 1954 (Conchostraca, Afrograptioidea): redescription and new combination to *Isaura olsoni* Bock from Venezuela and a new species from Argentina (Upper Jurassic). Alavesia 3, 11–24.
Gallego, O.F., Cabaleri, N.G., Armella, C., Volkheimer, W., Ballent, S., Martínez, S., Monferran, M., Silva Nieto, D.G., Páez, M.A., 2011. Paleontology, sedimentology and paleoenvironment of a new fossiliferous locality of the Jurassic Cañadón Asfalto Formation, Chubut Province, Argentina. J. S. Am. Earth Sci. 31, 54–68.
Gawthorpe, R.L., Leeder, M.R., 2000. Tectono-sedimentary evolution of active extensional basins. Basin Res. 12, 195–218.
Gregg, J.M., Sibley, D.F., 1984. Epigenetic dolomitization and the origin of xenotopic dolomite texture. J. Sediment. Res. 54, 908–931.
Hasiotis, S.T., Van Wagoner, J.C., Demko, T.M., Wellner, R.W., Jones, C.R., Hill, R.E., McCrimmon, G.G., Feldman, H.R., Drzewiecki, P.A., Patterson, P., Donovan, A.D., Geslin, J.K., 2006. Continental ichnology: using terrestrial and freshwater trace fossils for environmental and climatic interpretations. Cont. Trace Fossils 51, 1–53.
Hauser, N., Massimo, M., Cabaleri, N., Volkheimer, W., Armella, C., Gallego, O.F., Monferran, M.D., 2012. New U–Pb ages on a pyroclastic level from the Fosatti depocenter of the Jurassic Cañadon Asfalto basin, Chubut, Argentina. VIII South American Symposium On Isotope Geology. CDR, Medellín, Colombia.
Hay, R.L., 1966. Zeolites and zeolitic reactions in sedimentary rocks. Special Paper, Geological Society of America, 85. Universidad Nacional de Colombia, Boulder (130 pp.).
Iglesias, A., Artabe, A.E., Morel, A.M., 2011. The evolution of Patagonian climate and vegetation from the Mesozoic to the present. Biol. J. Linn. Soc. 103, 409–422.
Jaillard, B., Guyon, A., Maurin, A.F., 1991. Structure and composition of calcified roots, and their identification in calcareous soils. Geoderma 50, 197–210.
Knoll, A.H., 1985. Exceptional preservation of photosynthetic organisms in sicilified carbonates and silicified peats. Philos. Trans. R. Soc. Lond. B311, 111–122.
Košir, A., 2004. *Microcodium* revisited: root calcification products of terrestrial plants on carbonate–rich substrates. J. Sediment. Res. 74, 845–857.
Koukharsky, M., Quenardelle, S.V.D., Litvak, V., Page, S., Maisonnave, E.B., 2002. Plutonismo del Ordovícico inferior en el sector norte de la sierra de Macón, provincia de Salta. Rev. Asoc. Geol. Argent. 57, 182–194.
Kraus, M.J., Hasiotis, S.T., 2006. Significance of different modes of rhizolith preservation to interpreting paleoenvironmental and paleohydrologic settings: examples from Paleogene palaeosols, Bighorn Basin, Wyomi NG, U.S.A. J. Sediment. Res. 76, 633–646.
Lesta, P., 1968. Estratigrafía de la cuenca del Golfo de San Jorge. Actas 3ª Jornadas Geológicas Argentinas. Asociación Geológica Argentina, Buenos Aires, pp. 187–289.
Lesta, P., Ferello, R., 1972. Región extraandina de Chubut y norte de Santa Cruz. In: Leanza, A. (Ed.), Geología Regional Argentina. Academia Nacional Ciencias, Córdoba, pp. 601–653.
Lizuain, A., Silva Nieto, D., 1996. Estratigrafía mesozoica del río Chubut medio (sierra de Taquetrén). Provincia del Chubut. Actas 13ª Congreso Geológico Argentino and 3 Congreso de Exploración de Hidrocarburos, Buenos Aires, 1, pp. 479–493.
Martínez, S., Gallego, O.F., Cabaleri, N., 2007. Nueva fauna de moluscos de la Formación Cañadón Asfalto (Jurásico Medio a Superior) Chubut, Argentina. Ameghiniana 44, 96R (Suplemento).
Meléndez, N., Liesa, C.L., Soria, A.R., Meléndez, A., 2009. Lacustrine system evolution during early rifting: El Castellar Formation (Galve subbasin, Central Iberian Chain). Sediment. Geol. 222, 64–77.
Miall, A.D., 1996. The geology of fluvial deposits: sedimentary facies, basin analysis and petroleum geology. Springer-Verlag Inc., Berlin (582 pp.).
Monferran, M.D., Genise, J.F., Gallego, O.F., 2008. Capullos fósiles de Tricópteros del Jurásico Medio a Superior de la Patagonia Argentina. Resúmenes 7º Congreso Argentino de Entomología, Huerta Grande, Córdoba, p. 230.
Moore, D.M., Reynolds, R.C., 1997. X-ray Diffraction and the Identification and Analysis of Clay Minerals. Oxford University Press, New York (378 pp.).
Morsilli, M., Pomar, L., 2012. Internal waves vs. surface storm waves: a review on the origin ofhummocky cross-stratification. Terra Nova. http://dx.doi.org/10.1111/j.1365-3121.2012.01070.x.
Musacchio, E.A., 1995. Estratigrafía y micropalentología del Jurásico y el Cretácico en la comarca del Valle Medio del Río Chubut, Argentina. Actas 6º Congreso Argentino de Paleontología y Bioestratigrafía, Trelew, pp. 179–187.
Musacchio, E.A., Beros, C., Pujana, E.I., 1990. Microfósiles continentales del Jurásico y Cretácico del Chubut y su contribución a la bioestratigrafía de la Cuenca del Golfo de San Jorge. Argentina. In: Volkheimer, W. (Ed.), Bioestratigrafía de los Sistemas Regionales del Jurásico y Cretácico de América del Sur, 2. Comité Sudamericano del Jurásico y Cretácico, Mendoza, pp. 355–383.
Nullo, F., 1983. Descripción geológica de la Hoja 45c, Pampa de Agnia, provincia del Chubut. Boletín del Servicio Geológico Nacional, 199. Asociación Geológica Argentina, Buenos Aires, Argentina 1–94.
Orti, F., Rosell, L., Anadon, P., 2003. Deep to shallow lacustrine evaporates in the Libros Gypsum (southern teruel Basin, Miocene, NE Spain): an occurrence of pelletal gypsum rhythmites. Sedimentology 50, 361–386.
Ott, E., Volkheimer, W., 1972. *Paleospongilla chubutensis* n.g. et n.sp. – ein Süβwasserscwamm aus der Kreide Patagoniens. N. Jb. Geol. Paläont. (Abh.) 140 (1), 49–63.
Petrulevicius, J.F., 2007. A new species of Bittacidae sensu lato (Mecoptera) from the Callovian-Oxfordian: new Jurassic locality of insect body fossils from Patagonia, Argentina. Proceedings of the 4th International Congress of Paleoentomology. International Palaeoentomological Society, Vitoria-Gasteiz, Diputación Forai de Álava, Spain, p. 275.
Piatnitzky, C., 1936. Informe preliminar sobre el estudio geológico de la región situada al norte de los lagos Colhué Huapi y Musters. Yacimientos Petrolíferos Fiscales, Buenos Aires, (unpublished), 120 pp.
Platt, N., Wright, P., 1992. Palustrine carbonates and the Florida Everglades: towards an exposure index for the fresh-water environment. J. Sediment. Petrol. 62 (6), 1058–1071.
Quattrocchio, M.E., Volkheimer, W., Borromei, A.M., Martínez, M.A., 2011. Changes of the palynobiotas in the Mesozoic and Cenozoic of Patagonia: a review. Biol. J. Linn. Soc. 103, 380–396.
Rabassa, J., 2010. Gondwana paleolandscapes: term landscape evolution, genesis, distribution and age. Geociências 29, 541–557.
Ranalli, J.N., Peroni, G.O., Boggetti, D.A., Manolo, R., 2011. Cuenca Cañadón Asfalto. Modelo tectosedimentario. Actas 8º Congreso de Exploración y Desarrollo de Hidrocarburos. 1. Instituto Argentino del Petróleo y del Gas, Mar del Plata, pp. 185–215.
Ravazzoli, I.A., Sesana, F.L., 1997. Descripción Geológica de la Hoja 41c, Río Chico. Provincia de Río Negro. Boletín del Servicio Geológico Nacional, 148. SEGEMAR, Buenos Aires 1–79.
Rees, P.M., Ziegler, A.M., Valdes, P.J., 2000. Jurassic phytogeography and climates: new data and model comparisons. In: Huber, B.T., MacLeod, K.G., Wing, S.L. (Eds.), Warm Climates in Earth History. Cambridge University Press, Cambridge, pp. 297–318.
Remy, W., Remy, R., 1977. Die Floren des Erdaltertums. Verlag Glückauf GMBH, Essen (468 pp.).
Royer, D.L., 2006. CO_2-forced climate thresholds during the Phanerozoic. Geochim. Cosmochim. Acta 70, 5665–5675.
Salani, F.M., 2007. Aporte a la edad de la Formación Cañadón Asfalto, Chubut Argentina. Ameghiniana 44, 48R (Suplemento).
Sánchez, M.L., Calvo, J.O., Heredia, S., 2005. Paleoambientes de sedimentación del tramo superior de la Formación Portezuelo, Grupo Neuquén (Cretácico Superior), Los Barreales, provincia del Neuquén. Rev. Asoc. Geol. Argent. 60, 142–158.
Sanz-Montero, M.E., Rodríguez-Aranda, J.P., García del Cura, M.A., 2008. Dolomite–silica stromatolites in Miocene lacustrine deposits from the Duero Basin, Spain: the role of organotemplates in the precipitation of dolomite. Sedimentology 55, 729–750.
Sheppard, R.A., Gude, A.J., 1969. Diagenesis in tuffs of the Barstow Formation, Mud Hills, San Bernardino County, California. US Geol. Surv. Prof. Pap. 634.
Shiraishi, F., Reimer, A., Bisset, A., De Beer, D., Arp, G., 2008. Microbial effects on biofilm calcification, ambient water chemistry and stable isotope records in a highly supersaturated setting (Westerhöfer Bach, Germany). Palaeogeogr. Palaeoclimatol. Palaeoecol. 262, 91–106.
Silva Nieto, D., 2005. Hoja Geológica 4369-III, Paso de Indios. Escala 1:250.000. Boletín del Instituto de Geología y Recursos Minerales, Servicio Geológico Minero Argentino, Buenos Aires, 265, 1–72.
Silva Nieto, D., Cabaleri, N., Armella, C., Volkheimer, W., Gallego, O., 2007. Hipótesis sobre la evolución tecto-sedimentaria de la Formación Cañadón Asfalto Provincia del Chubut. Ameghiniana 44, 67R (Suplemento).
Spalletti, L.A., Franzese, J.R., 2007. Mesozoic paleogeography and paleoenvironmental evolution of Patagonia (southern South America). In: Gasparini, Z., Leonardo, S., Coria, R. (Eds.), Patagonian mesozoic reptiles. Indiana University Press, Bloomington, pp. 29–49 (Chapter 2).
Stipanicic, P.N., Rodrigo, F., Baulíes, O., Martínez, C., 1968. Las formaciones presenonianas en el dominio del Macizo Nordpatagónico y regiones adyacentes. Rev. Asoc. Geol. Argent. 23, 67–98.
Surdam, R.C., Sheppard, R.A., 1978. Zeolitas in saline, alkaline-lake deposits. In: Sand, L.B., Humpton, F.A. (Eds.), Natural Zeolites Occurrence, Properties, Use. Pergamon Press, Press Elmsford, New York, pp. 145–174.
Tasch, P., Volkheimer, W., 1970. Jurassic conchostracans from Patagonia. Univ. Kans. Paleontol. Contrib. 50, 1–23.
Turner, J., 1983. Descripción geológica de la Hoja 44d Colan Conuhé, provincia del Chubut. Boletín del Servicio Geológico Nacional, 197. Asociación Paleontológica Argentina, Buenos Aires 1–78.
Turner, C.E., Peterson, F., 2004. Reconstruction of the Upper Jurassic Morrison Formation extinct ecosystem—a synthesis. Sediment. Geol. 167, 309–355.
Vallati, P., 1986. Conchostracos Jurásicos de la Provincia de Chubut, Argentina. Actas 4º Congreso Argentino de Paleontología y Bioestratigrafiía, Mendoza, pp. 29–38.
Vázquez-Urbez, M., Arenas, C., Pardo, G., 2002. Facies fluvio-lacustres de la Unidad superior de la Muela de Borja (Cuenca del Ebro): modelo sedimentario. Rev. Soc. Geol. Esp. 15, 41–54.
Volkheimer, W., Melendi, D., 1976. Palinomorfos como fósiles guía. Tercera parte: Técnicas de laboratorio palinológico. Rev. Miner. Geol. Miner. 34, 19–30.
Volkheimer, W., Quattrocchio, M., Cabaleri, N.G., García, V., 2008. Palynology and paleoenvironment of the Jurassic lacustrine Cañadón Asfalto Formation at Cañadón Lahuincó locality, Chubut province, central Patagonia, Argentina. Rev. Esp. Micropaleontol. 40, 77–96.
Wilkin, R.T., Barnes, H.L., 1998. Solubility and stability of zeolites in aqueous solution: I. Analcime, Na-, and K-clinoptilolite. Am. Mineral. 83, 746–761.
Wright, V.P., 1994. Paleosols in shallow marine carbonate sequences. Earth Sci. Rev. 35, 367–395.